



Dust radiative effects  
over the  
Mediterranean

P. Nabat et al.

This discussion paper is/has been under review for the journal Atmospheric Chemistry and Physics (ACP). Please refer to the corresponding final paper in ACP if available.

# Dust aerosol radiative effects during summer 2012 simulated with a coupled regional aerosol–atmosphere–ocean model over the Mediterranean

P. Nabat<sup>1</sup>, S. Somot<sup>1</sup>, M. Mallet<sup>2</sup>, M. Michou<sup>1</sup>, F. Sevault<sup>1</sup>, F. Driouech<sup>3</sup>,  
D. Meloni<sup>4</sup>, A. Di Sarra<sup>4</sup>, C. Di Biagio<sup>5</sup>, P. Formenti<sup>5</sup>, M. Sicard<sup>6</sup>, J.-F. Léon<sup>2</sup>, and  
M.-N. Bouin<sup>7</sup>

<sup>1</sup>Météo-France, CNRM-GAME, Centre National de Recherches Météorologiques, UMR3589, Toulouse, France

<sup>2</sup>Laboratoire d'Aérodologie, Toulouse, France

<sup>3</sup>Direction de la Météorologie Nationale, Casablanca, Morocco

<sup>4</sup>Laboratory for Earth Observations and Analyses, ENEA, Rome, Italy

<sup>5</sup>Laboratoire Interuniversitaire des Systèmes Atmosphériques (LISA), UMR7583 – CNRS, Créteil, France

<sup>6</sup>Universitat Politècnica de Catalunya, Barcelona, Spain

<sup>7</sup>Météo-France, CMM, Centre de Météorologie Marine, Brest, France

Title Page

Abstract

Introduction

Conclusions

References

Tables

Figures



Back

Close

Full Screen / Esc

Printer-friendly Version

Interactive Discussion



Received: 1 July 2014 – Accepted: 15 September 2014 – Published: 2 October 2014

Correspondence to: P. Nabat (pierre.nabat@meteo.fr)

Published by Copernicus Publications on behalf of the European Geosciences Union.

**ACPD**

14, 25351–25410, 2014

---

**Dust radiative effects  
over the  
Mediterranean**

P. Nabat et al.

---

Title Page

Abstract

Introduction

Conclusions

References

Tables

Figures



Back

Close

Full Screen / Esc

Printer-friendly Version

Interactive Discussion



## Abstract

The present study investigates the effects of aerosols on the Mediterranean climate daily variability during summer 2012. Simulations have been carried out using the coupled regional climate system model CNRM-RCSM5 which includes prognostic aerosols, namely desert dust, sea salt, organic, black-carbon and sulfate particles, in addition to the atmosphere, land surface and ocean components. An evaluation of the dust aerosol scheme of CNRM-RCSM5 has been performed against in-situ and satellite measurements. This scheme shows its ability to reproduce the spatial and temporal variability of aerosol optical depth (AOD) over the Mediterranean region in summer 2012. Observations from the TRAQA/ChArMEx campaign also show that the model correctly represents dust vertical and size distributions. Thus CNRM-RCSM5 can be used for aerosol–climate studies over the Mediterranean. Here we focus on the effects of dust particles on surface temperature and radiation daily variability. Surface short-wave aerosol radiative forcing variability is found to be more than twice higher over regions affected by dust aerosols, when using a prognostic aerosol scheme instead of a monthly climatology. In this case downward surface solar radiation is also found to be better reproduced according to a comparison with several stations across the Mediterranean. Moreover, the radiative forcing due to the dust outbreaks also causes an extra cooling in land and sea surface temperatures. A composite study has been carried out for 14 stations across the Mediterranean to identify more precisely the differences between dusty days and the set of all the days. Observations show that dusty days receive less radiation at the surface and are warmer than average because of southwesterly fluxes often generating dust outbreaks. Only the simulation using the prognostic aerosol scheme is found to reproduce the observed intensity of the dimming and warming on dusty days. Otherwise, the dimming is underestimated and the warming overestimated.

## Dust radiative effects over the Mediterranean

P. Nabat et al.

Title Page

Abstract

Introduction

Conclusions

References

Tables

Figures



Back

Close

Full Screen / Esc

Printer-friendly Version

Interactive Discussion



## 1 Introduction

Numerous and various aerosols affect the Mediterranean basin (Lelieveld et al., 2002), located at the crossroads of air masses carrying both natural (desertic particles, sea-salt, volcanic ashes, etc.) and anthropogenic (black carbon, sulfate, etc.) particles. Because of their microphysical and optical properties, these aerosols can have strong effects on the regional radiative budget (e.g. Bergamo et al., 2008), with ensuing impact on climate (Zanis et al., 2012; Spyrou et al., 2013; Nabat et al., 2014), and ecosystems of the Mediterranean (Guieu et al., 2010). Among these aerosols, the Saharan desert dust particles represent an important contribution of aerosols for this region (Barnaba and Gobbi, 2004; Nabat et al., 2013). Indeed, dust particles coming from suspension, saltation and creeping processes associated with wind erosion, can move from northern Africa to the Mediterranean Sea and Europe (Moulin et al., 1997; Papadimas et al., 2008; Gkikas et al., 2013). These dust outbreaks are mainly driven by the synoptic meteorological conditions (Gkikas et al., 2012): they are more frequent in the eastern basin in winter and spring, in the central basin in spring and in the western basin in summer (Moulin et al., 1998). The ChArMEx initiative (Chemistry-Aerosol Mediterranean Experiment, <http://charmex.lsce.ipsl.fr>) has been launched for a few years in the framework of the MISTRALS (Mediterranean Integrated STudies at Regional And Local Scales) program, in order to improve our knowledge of aerosols and their impacts on climate in the Mediterranean. Thus, in early summer 2012, the ChArMEx/TRAQA (TRansport and Air QuAlity) campaign focused on the characterization of the air pollution masses over the Mediterranean basin through the study of representative case studies. A particularly intense dust event has been measured at the end of June with different observation means (balloons, aircraft, surface and remote-sensing measurements), and consequently represents a documented case to evaluate the ability of climate models to reproduce this kind of events and their effects on climate. The aim of the present work is consequently to evaluate the direct and semi-direct effects of

### Dust radiative effects over the Mediterranean

P. Nabat et al.

Title Page

Abstract

Introduction

Conclusions

References

Tables

Figures



Back

Close

Full Screen / Esc

Printer-friendly Version

Interactive Discussion





**Dust radiative effects  
over the  
Mediterranean**

P. Nabat et al.

Title Page

Abstract

Introduction

Conclusions

References

Tables

Figures



Back

Close

Full Screen / Esc

Printer-friendly Version

Interactive Discussion



In addition, as the Mediterranean is also characterized by local winds, complex coastlines and orography, high resolution modelling is needed to correctly reproduce the atmospheric circulation (Gibelin and Déqué, 2003; Gao et al., 2006; Giorgi and Lionello, 2008).

From our knowledge, none of these regional models can have at the same time ocean–atmosphere coupling and prognostic aerosol schemes. In the present study, a new version of the coupled regional climate model system (RCSM) of the CNRM, called CNRM-RCSM5, has been developed, including an aerosol prognostic scheme derived from the GEMS/MACC project (Morcrette et al., 2009; Michou et al., 2014), in addition to the atmosphere, ocean and land-surface components. This new model tool thus complies with all the criteria mentioned above, and should be able to help us to evaluate the direct and semi-direct effects of dust aerosols at the daily time scale. The data brought by the TRAQA campaign also enable a first evaluation of the dust aerosol scheme before assessing the aerosol impact on climate. Besides, including the other aerosol species allows a comparison of total aerosol optical depth with remote-sensing measurements. The question of the difference between the use of climatologic and prognostic aerosols in this model will also be raised.

After a description of the aerosol scheme in Sect. 2 and its evaluation in Sect. 3, the aerosol impact on climate is studied in Sects. 4 and 5, before the concluding remarks in Sect. 6.

## 2 Methodology

### 2.1 The CNRM-RCSM5 model

Four different components are included in this regional climate model system: the atmosphere with the regional climate model ALADIN-Climate (Déqué and Somot, 2008; Colin et al., 2010), the ocean with the regional model NEMOMED8 (Beuquier et al., 2010), the land-surface with the model ISBA (Noilhan and Mahfouf, 1996) and the



**Dust radiative effects  
over the  
Mediterranean**

P. Nabat et al.

[Title Page](#)[Abstract](#)[Introduction](#)[Conclusions](#)[References](#)[Tables](#)[Figures](#)[Back](#)[Close](#)[Full Screen / Esc](#)[Printer-friendly Version](#)[Interactive Discussion](#)

scheme has been included, adapted from the GEMS/MACC aerosol scheme (Morcrette et al., 2009; Benedetti et al., 2011; Michou et al., 2014). It includes the same five aerosol species that can be directly emitted from the surface for dust and sea-salt particles, or from external emission datasets for black carbon, organic matter and sulfate precursors. The spatial domain of our simulations has consequently been extended compared to the previous study of Nabat et al. (2014), in order to include all the sources generating aerosols that can be transported over the Mediterranean basin. No aerosol is indeed included in the lateral boundary forcing.

Sea salt aerosols are generated by wind stress on ocean surface, either because of air bubbles bursting at the sea surface, or from spume droplets directly torn off the wave crests by the wind. Guelle et al. (2001) have reviewed different approaches to model these processes. The current formulation used in ALADIN-Climate is based on the studies of Guelle et al. (2001) and Schulz et al. (2004), that provide surface mass fluxes at 80 % relative humidity depending on 10 m-wind, integrated for the three size bins defined in the scheme: 0.03 to 0.5  $\mu\text{m}$ , 0.5 to 5  $\mu\text{m}$  and 5 to 20  $\mu\text{m}$ . Note that the size distribution of emitted sea salt also depends on other factors such as the sea surface temperature (Jaeglé et al., 2011), which are not taken into account in this current version.

Dust emission processes depend on several factors such as soil characteristics (chemical composition, humidity, roughness) and surface wind speed. In the GEMS/MACC scheme, the dust parameterization follows Ginoux et al. (2001), that propose a simplified formulation of dust emission, based on the wind speed and thresholds according to the fraction of bare soil and soil moisture. In ALADIN-Climate, this function has been replaced by the Marticorena and Bergametti (1995) parameterization, that takes into account more soil characteristics coming from the ECOCLIMAP database (Masson et al., 2003), which provides information on the erodible fraction and the sand and clay fractions, allowing a classification of the soil textures. After the determination of an erosion threshold based on the soil distribution, the soil moisture and the roughness caused by nonerodible elements, the horizontal saltation flux is cal-

---

**Dust radiative effects  
over the  
Mediterranean**P. Nabat et al.

---

[Title Page](#)[Abstract](#)[Introduction](#)[Conclusions](#)[References](#)[Tables](#)[Figures](#)[Back](#)[Close](#)[Full Screen / Esc](#)[Printer-friendly Version](#)[Interactive Discussion](#)

culated, proportionally to the third power of the wind friction velocity. The vertical flux is then inferred from this saltation flux, according to an empirical relationship given by Marticorena and Bergametti (1995), which notably depends on the soil clay content. The emitted dust size distribution is based on the work of Kok (2011). More details about this dust emission parameterization can be found in Nabat et al. (2012), who have used the same dust emission scheme in RegCM4. Once emitted dust particles are integrated in the three dust size bins of the scheme: 0.01 to 1.0  $\mu\text{m}$ , 1.0 to 2.5  $\mu\text{m}$  and 2.5 to 20  $\mu\text{m}$ .

The external emission datasets for the three other aerosol types come from Lamarque et al. (2010), who have provided inventories at 0.5° resolution of different species for climate models. These inventories include numerous sectors such as energy production, industries, domestic activities, agriculture, transport and fires. Organic and black carbon particles are separated between hydrophile and hydrophobic particles. SO<sub>2</sub> emitted particles can be transformed in SO<sub>4</sub>, but 5 % of them are directly emitted as SO<sub>4</sub> aerosols (Benkovitz et al., 1996). Volcanic sulfur emissions are also included, as well as DMS particles from oceans (see Michou et al., 2014).

All these aerosols gathered in 12 bins are then transported in the atmosphere, before possible dry or wet deposition. More details about transport and deposition can be found in Morcrette et al. (2009). Optical properties (single scattering albedo and asymmetry factor) are fixed for each aerosol type, as defined in Nabat et al. (2013). The complexity of this aerosol scheme is similar to the one used in RegCM, but it does not include detailed chemical processes that can be found in COSMO-ART (Vogel et al., 2009). However it enables our model to keep a low cost of calculations, so that multi-annual simulations could be carried out for aerosol–climate studies.

## 2.3 Simulations

Three simulations have been carried out with CNRM-RCSM5, driven by the ERA-Interim reanalysis (Dee et al., 2011) as initial and lateral boundary forcing. The PROG simulation includes the whole aerosol prognostic scheme described previously. The

## Dust radiative effects over the Mediterranean

P. Nabat et al.

Title Page

Abstract

Introduction

Conclusions

References

Tables

Figures



Back

Close

Full Screen / Esc

Printer-friendly Version

Interactive Discussion



PROG-M simulation uses monthly AOD provided by PROG, so that PROG and PROG-M share the same average aerosol content at the monthly scale. The NO simulation does not include any aerosols. Comparisons between these simulations will enable to estimate the aerosol effects on the radiative budget and regional climate, and the implications of using prognostic aerosol schemes instead of monthly climatologies. The three simulations cover the summer 2012 period from 1 June to 31 August. A one-month spin-up period has been performed for each simulation in order to have realist aerosol concentrations on 1 June.

### 2.4 Observation data

For the evaluation of the aerosols and their direct radiative effects, different observed datasets are used in the present work.

Simulated AOD is compared to satellite data from the MODerate resolution Imaging Spectroradiometer (MODIS, collection 5.1, standard and Deep Blue algorithms, 1° resolution, Tanré et al., 1997; Levy et al., 2007), the Multiangle Imaging SpectroRadiometer (MISR, Level3, Kahn et al., 2005, 2010) and the SEVIRI radiometer onboard the geostationary satellite Meteosat Second Generation (MSG). For the latter instrument, we use the algorithm of Carrer et al. (2010), which provides high-resolution AOD over both ocean and land surfaces. Nowadays, this algorithm is being implemented on the production chain of the ICARE thematic center (<http://www.icare.univ-lille1.fr>) under the name of AERUS-GEO (Aerosol and surface albEdo Retrieval Using a directional Splitting method-application to GEO data).

Ground-based observations from 30 stations of the AERosol RObotic NETwork (AERONET, Holben et al., 1998, 2001) will also be considered (Fig. 1). These sun-photometer observations provide high-quality data (Level 2.0), which have been downloaded from the AERONET website (<http://aeronet.gsfc.nasa.gov>). All AOD data have been calculated at 550 nm using the Angstrom coefficient when necessary, to make comparisons and evaluation easier.

**Dust radiative effects  
over the  
Mediterranean**

P. Nabat et al.

Title Page

Abstract

Introduction

Conclusions

References

Tables

Figures



Back

Close

Full Screen / Esc

Printer-friendly Version

Interactive Discussion



The TRAQA campaign has also provided interesting observations for dust aerosols, namely vertical profiles from lidar instruments in Barcelona and San Giuliano (Cor- sica). The Barcelona lidar system is part of the ACTRIS/EARLINET network (Aerosols, Clouds, and Trace gases Research InfraStructure Network/European Aerosol Re- search Lidar Network, Pappalardo et al., 2014). The extinction coefficient profiles were retrieved by means of the two-component elastic lidar inversion algorithm constrained with the AERONET sun-photometer-derived AOD (Reba et al., 2010). In San Giuliano (42.28° N, 9.51° E), aerosol vertical profiles were acquired with a 355 nm backscattering lidar. The aerosol extinction coefficient profiles are estimated using the Klett's method and a fix lidar ratio (Léon et al., 2014) from hourly averaged attenuated range-corr- ed lidar signals. Besides, an ATR-42 research flight operated by SAFIRE (Service des Avions Français Instrumentés pour la Recherche en Environnement) has also been realized during the TRAQA campaign. This study uses the airborne data from the Pas- sive Cavity Aerosol SPectrometer (PCASP), which measures particles between 0.1 and 3.2  $\mu\text{m}$ .

In addition, the Météo-France and AEMET networks have provided daily radiation and 2 m-temperature measurements (see Fig. 1). Radiation measurements have been completed by the stations of Sede-Boker (SED, SolRad-Net network, AERONET web- site), Lampedusa (LAM, coll. ENEA) and two Météo-France buoys located in the Gulf of Lions (LIO) and near the French Riviera (AZU). Lampedusa and the two buoys also provide sea surface temperature (SST) measurements. All the fourteen stations providing surface radiation and temperature have been added in Fig. 1 (red crosses). It is worth mentioning that available data is provided by stations that are located for most of them in the western Mediterranean. However, in summer, most of the dust outbreaks occur in this region because of frequent low pressure systems over Morocco that favour the dust export over the western Mediterranean (Moulin et al., 1998; Gkikas et al., 2012).

Besides, the MACC reanalysis (Morcrette et al., 2009) is also used in the present work, as a means of evaluating the CNRM-RCSM5 simulations. This reanalysis in- cludes data assimilation from the MODIS instrument (AOD).

### 3 Evaluation of the simulated aerosols

#### 3.1 Aerosol optical depth

The average AOD simulated by PROG in summer 2012 is presented in Figs. 2 and 3, respectively for the five aerosol types, and for total AOD. Figure 3 also presents the average AOD for summer 2012 for three satellite products (MODIS, MISR and AERUS-GEO) as well as the MACC reanalysis (Morcrette et al., 2009; Benedetti et al., 2011). The general spatial pattern shows a good agreement between satellites, MACC and CNRM-RCSM5. The highest values (up to 1.5) are indeed found over northern Africa and Arabian peninsula, where dust aerosols are emitted, while anthropogenic particles, especially sulfate and organic matter, are responsible for local maxima in Europe. The Mediterranean Sea, located between both sources, is also affected by moderate AOD, ranging from 0.15 to 0.3, from the north-east to the south-west. Sea-salt particles are essentially simulated over the Atlantic ocean, as well as the western Mediterranean Sea in lower quantities.

In greater detail, some differences can be noted between the model and satellite data. CNRM-RCSM5 AOD is closer to MISR over northern Africa, where a large zone of AOD higher than 0.5 can be identified in both datasets, while MODIS and especially AERUS-GEO show lower AOD. Similar conclusions can be drawn for the Arabian peninsula. Dust export over the Atlantic ocean is on the contrary in very good agreement between the five products (AOD between 0.5 and 0.7). Over western and central Europe, MISR AOD is lower than MODIS, AERUS-GEO, MACC and CNRM-RCSM5. Large differences in AOD are also present in Eastern Europe and Russia, where MODIS shows higher AOD than the other datasets. However, this region is in the limit of the domain seen by SEVIRI (lower values in AERUS-GEO), and is also close to the border of the domain used in CNRM-RCSM5, so that aerosols over this region may come from outside the domain. Finally, AOD over the northern Atlantic ocean is higher in CNRM-RCSM5 and MACC than in satellite products, but the presence of numerous clouds in this area limits the quality of the satellite data there.

## Dust radiative effects over the Mediterranean

P. Nabat et al.

Title Page

Abstract

Introduction

Conclusions

References

Tables

Figures



Back

Close

Full Screen / Esc

Printer-friendly Version

Interactive Discussion



**Dust radiative effects  
over the  
Mediterranean**

P. Nabat et al.

[Title Page](#)[Abstract](#)[Introduction](#)[Conclusions](#)[References](#)[Tables](#)[Figures](#)[Back](#)[Close](#)[Full Screen / Esc](#)[Printer-friendly Version](#)[Interactive Discussion](#)

Averages for summer 2012 are given in Table 1, for CNRM-RCSM5 and different model and satellite datasets: the MACC reanalysis, the AOD climatology from Nabat et al. (2013), named NAB13 thereafter, MODIS, MISR and AERUS-GEO. NAB13 and MACC, which present AOD components for each aerosol type, are based on both model and satellite data for the first one, and on model and data assimilation for the second one. NAB13, which gives reliable estimations of the different AOD components, is only available on the 2003–2009 period, so that the average over this period with the minimum and maximum values have been indicated. Averages have been calculated on the three domains defined in Nabat et al. (2013): Europe, the Mediterranean Sea and northern Africa.

Over Europe, CNRM-RCSM5 is very close to NAB13 for total AOD (0.18 on average) and the five aerosol types, even if the sharing between organic matter and sulfate aerosols is slightly different. MACC simulate more dust and sulfate particles, but the three satellite data have lower AOD (between 0.15 and 0.16), so that CNRM-RCSM5 AOD is median. Over the Mediterranean Sea, a good agreement is shown between CNRM-RCSM5 (0.23 for total AOD), MACC (0.24) and NAB13 (0.23). In addition, the proportion between the different aerosol types is similar in the three datasets. However, as in Europe, satellite data have lower AOD (between 0.18 and 0.22).

More variability is noted with regards to AOD over northern Africa, notably because of the dust component. CNRM-RCSM5 shows higher AOD (0.45) than NAB13 (0.41), MACC (0.32) and the satellite data (between 0.21 and 0.33). However, interannual variability is stronger in this region as shown by the larger amplitude in NAB13 (0.33–0.44). Moreover, MACC does not assimilate AOD over the Sahara because the standard algorithm of MODIS cannot retrieve AOD on bright surface, so that an underestimation of dust aerosols in MACC had been identified (Nabat et al., 2013).

This evaluation has been completed by a comparison to ground-based observations from the AERONET network that provide accurate AOD measurements. Over 30 stations around the Mediterranean basin (see Fig. 1), the mean bias of CNRM-RCSM5 is 0.02, against  $-0.03$  for AERUS-GEO, 0.04 for MODIS,  $-0.07$  for MISR and  $-0.09$

for MACC. Considering only the stations to the south of 33° N, CNRM-RCSM5 has also the lowest bias (0.03) compared to AERUS-GEO (−0.06), MODIS (0.04), MISR (−0.07) and MACC (−0.10).

As a summary, Table 2 presents the spatial correlations between these five products. All the correlations are higher than 0.6, confirming the general agreement. CNRM-RCSM5 correlations are comparable to the scores of the satellite products when compared together, indicating its ability to reproduce the spatial patterns of AOD over this region.

As far as the daily scale is concerned, Fig. 4 shows four temporal series across the Mediterranean basin, respectively at Oujda (a, Morocco, number 10 in Fig. 1), Mallorca (b, Spain, 2), Frioul (c, France, 8) and Lampedusa (d, Italy, 1). All these series show high daily variability, because of frequent dust outbreaks in this season. The spectral nudging technique used in CNRM-RCSM5 enables to reproduce the true chronology of the synoptic meteorological conditions as shown in Herrmann et al. (2011), which is useful for driving dust emission. in the present work. As a result, the model is able to reproduce the intensity and the chronology of most AOD peaks, such as those observed in Oujda (18 June, 25 July) in Mallorca (19 June, 9 July, 10 August), Frioul (28 June, 19 August) and Lampedusa (21 June, 13 August). However, CNRM-RCSM5 sometimes overestimate some dust events (e.g. 19 June in Frioul, 15 June in Lampedusa), but these differences remain in minority.

Similar comparisons have been realized for 30 AERONET stations (see their locations on Fig. 1), the results are presented in a Taylor diagram (Fig. 5, adapted to daily time series from Taylor, 2001). This diagram represents three statistics: the correlation coefficient is the azimuth angle, the radial distance from the origin is the standard deviation normalised by observations, and the distance to the “REF” point on the x-axis is the root-mean-square error (RMSE). The average temporal correlation coefficient for CNRM-RCSM5 is 0.70, while the ratio between simulated and observed standard deviations is 1.01, revealing the ability of the aerosol scheme to reproduce AOD daily variability. This scores are close to MODIS and AERUS-GEO, whose standard devia-

## Dust radiative effects over the Mediterranean

P. Nabat et al.

[Title Page](#)[Abstract](#)[Introduction](#)[Conclusions](#)[References](#)[Tables](#)[Figures](#)[Back](#)[Close](#)[Full Screen / Esc](#)[Printer-friendly Version](#)[Interactive Discussion](#)



**Dust radiative effects  
over the  
Mediterranean**

P. Nabat et al.

Title Page

Abstract

Introduction

Conclusions

References

Tables

Figures



Back

Close

Full Screen / Esc

Printer-friendly Version

Interactive Discussion



in terms of extinction coefficient in Barcelona at 532 nm and in San Giuliano at 355 nm. Dust aerosols first reach Spain on 27 June, transported in the mid-troposphere, as noted in the profile between 2000 and 5000 m with a maximum extinction ( $0.18 \text{ km}^{-1}$ ) at 3500 m. The two-component elastic lidar inversion algorithm constrained with an AERONET AOD of 0.32 gave a column-equivalent lidar ratio of 54 sr. This value is in the range of 50–70 sr established by Tesche et al. (2009) of desert dust lidar ratio observations by Raman lidar, which makes us confident with the result of the lidar inversion. The altitude of these dust particles is similar in CNRM-RCSM5, despite an underestimation of the intensity of the dust outbreak and a slight overestimation in the higher layers. Under this dust layer, the presence of sulfate aerosols is noted in the model, with an extinction coefficient close to observations ( $0.03 \text{ km}^{-1}$ ). In San Giuliano, where the dust plume has arrived three days later, its altitude is also similar in CNRM-RCSM5 and observations: between 2000 and 5000 m. As in Barcelona, extinction is slightly overestimated in the high troposphere (above 6500 m).

Size distribution is also an essential physical parameter for aerosol–climate studies, as optical properties depend on the particle size. Figure 7 presents the size distribution observed during a sounding realized by the ATR42 during the TRAQA campaign, as well as the simulated distribution. Note that the bin scheme used in CNRM-RCSM5 does not enable to reproduce exactly the observed distribution, but the division in 3 bins for dust particles notably can still be evaluated. This sounding took place in the Mediterranean Sea ( $43.05^\circ \text{ N}$ ,  $9.55^\circ \text{ E}$ ) on 29 June, when the dust plume has been transported over this area. In the lower layers, a first maximum is observed in the smallest particles (around  $0.1 \mu\text{m}$ ), probably due to sulfate aerosols, as represented by CNRM-RCSM5. The observed distribution shows that mass concentration is higher for larger particles, especially between 2000 and 4000 m, where dust aerosols are located. This distribution is simulated by CNRM-RCSM5, notably between 2000 and 3000 m. Above 3000 m, coarse particles (larger than  $2.0 \mu\text{m}$ ) are underestimated. However, these particles have less impact on extinction than submicronic particles, but they could play a role in other processes (e.g. deposition).



Africa. Consequently dust particles show high variability over the Mediterranean basin that PROG-M cannot take into account contrary to PROG. The only daily variations of DRF in PROG-M are due to cloud cover variations, as the aerosol effect can be partially masked by the presence of clouds.

Daily temporal series in Oujda, Frioul, Lampedusa and Mallorca (Fig. 8c) confirm that aerosol forcing variability is more important in PROG than in PROG-M. For example in Mallorca, aerosol DRF ranges from  $-70$  to  $-5 \text{ W m}^{-2}$  in PROG but only  $-30$  to  $-10 \text{ W m}^{-2}$  in PROG-M. Indeed, during a given month, AOD can vary in PROG at each time step, but is constant in PROG-M. DRF can reach highest negative values in PROG whenever AOD peaks (Figs. 4 and 8). Consequently, PROG-M misses the strong dust outbreaks that can occur over the Mediterranean basin. Compared to estimations from literature such as the studies of Di Sarra et al. (2008) and Di Biagio et al. (2010) who have respectively found an average DRF of  $-30$  and  $-26 \text{ W m}^{-2}$  in Lampedusa, the values given by CNRM-RCSM5 have the same order of magnitude, even if they can reach largest forcings. Note also that the Atlantic ocean under the influence of dust export shows the highest variability.

## 4.2 Surface radiation

As dust outbreaks cause high DRF values and variability in PROG, consequences on climate might be expected, first on surface radiation. The idea is therefore to have colocalized measurement of AOD, shortwave radiation and 2 m temperature, which is hard to obtain. A few ground-based measurements are thus available to evaluate the ability of the model to reproduce the observed radiation. Here an evaluation of solar surface radiation (SSR) is presented in details for two stations representative of the Mediterranean basin, namely Lampedusa and Murcia. Lampedusa is located on an island close to dust-emitting regions where clear-sky conditions are frequent in summer, while Murcia is located in southeastern Spain, where more clouds are observed. Figure 9 presents the daily series of AOD and downward SSR in Lampedusa, observed and simulated by PROG, PROG-M and NO.

## Dust radiative effects over the Mediterranean

P. Nabat et al.

Title Page

Abstract

Introduction

Conclusions

References

Tables

Figures



Back

Close

Full Screen / Esc

Printer-friendly Version

Interactive Discussion



**Dust radiative effects  
over the  
Mediterranean**

P. Nabat et al.

Title Page

Abstract

Introduction

Conclusions

References

Tables

Figures



Back

Close

Full Screen / Esc

Printer-friendly Version

Interactive Discussion



NO is the only CNRM-RCSM5 simulation to have a high bias against observed radiation ( $+18.0 \text{ W m}^{-2}$ ), compared to PROG-M ( $-6.0 \text{ W m}^{-2}$ ) and PROG ( $-3.5 \text{ W m}^{-2}$ ), due to the absence of aerosols in NO. While the aerosol climatology is enough to reduce the bias in PROG-M, PROG has the highest temporal correlation (0.87 against 0.81 for NO and 0.85 for PROG-M), and its standard deviation is the closest to observations (a ratio of 0.88 against 0.74 both for NO and PROG-M). Indeed, PROG-M and NO clearly miss some variations of SSR. When AOD is high (e.g. 21 June, 3–12 July, 29 July, 7 August), PROG-M and NO overestimate SSR, and inversely when AOD is low (e.g. 24 June, 20 July, 10 August) but only for PROG-M as NO benefits in this case from the absence of aerosols. ERA-Interim, which has a monthly aerosol climatology as in PROG-M, except that the aerosol climatology used in ERA-Interim (Tegen et al., 1997) is probably less realistic, also simulates radiation variations lower than observed. As a result, the effect of aerosols on surface radiation can easily be identified in Lampedusa, where cloud cover is generally low (see its variations in Fig. 9).

In Murcia, more affected by clouds than Lampedusa, similar results have been found. Figure 10 presents the same series as in Lampedusa in Fig. 9. NO is still the only simulation to have a high bias ( $+25.7 \text{ W m}^{-2}$ ) compared to PROG-M, PROG and ERA-Interim (lower than  $7 \text{ W m}^{-2}$ ). The remaining bias could be attributed to a lack of cloud cover in the model. The temporal correlation (0.77) and the standard deviation ratio (0.95) of PROG are higher than PROG-M and NO. The evolution of AOD also enables to justify the role of aerosols in the higher scores obtained by PROG. Indeed, the peaks in AOD generally correspond to minima in surface radiation in PROG (e.g. 18 June, 28 June, 28 July). In several of these cases (notably end July), PROG is the only simulation to reproduce the observed radiation. ERA-Interim, which has only a monthly aerosol climatology (Tegen et al., 1997), misses these minima in radiation.

Besides, PROG is also closer to SSR measurements when the atmospheric aerosol content is close to zero. Indeed, in case of clean air without aerosols, more radiation can reach the surface, as illustrated between 10 June and 14 June when PROG-M and ERA-Interim underestimate surface radiation because of their aerosol climatology.

Note finally that when PROG does not have the true aerosol content (e.g. 4 June), errors can also be found in radiation.

As a result, these comparisons in Lampedusa and Murcia show that the prognostic aerosol scheme used in PROG enables to better reproduce the evolution of surface radiation, that cannot be done properly with an aerosol climatology. This conclusion drawn from the series in Lampedusa and Murcia is also checked in other stations. Table 3 presents the scores obtained by the different simulations in 14 stations across the Mediterranean basin (see Table 5). On average, the bias is reduced both in PROG and PROG-M, reaching a level close to ERA-Interim (between 11 and 13 W m<sup>-2</sup>). A net improvement is noted in temporal correlation, since it is higher in PROG than in PROG-M and NO in every station. Daily variability in SSR is also higher in PROG for most stations, representing an improvement compared to observations except where this variability was already overestimated (e.g. Ajaccio). It is worth mentioning that in Sede-Boker PROG is getting closer to observations by reducing SSR variability. A misrepresentation of cloud processes could also explain some of the discrepancies with observations. The lack of cloud cover in CNRM-RCSM shown in Nabat et al. (2014) could explain the remaining bias. ERA-Interim that does not have the daily aerosol variations and consequently misses some peaks in surface radiation, succeeds in getting a high average correlation coefficient (0.79) probably because of a better representation of clouds. Moreover, changes in water vapour column amount may also affect the SSR to a lesser extent.

### 4.3 Land surface temperature

Once the impact of aerosols on surface radiation has been proven in the previous section, an effect on 2 m-temperature (T2m) could also be expected. Figure 11a presents the average difference between PROG-M and NO (top) and PROG and PROG-M (bottom) for summer 2012. As shown in Nabat et al. (2014), compared to NO, a general cooling is observed in PROG-M, due to the presence of aerosols that scatter and absorb incident solar radiation, preventing it from reaching the surface. This cooling is

## Dust radiative effects over the Mediterranean

P. Nabat et al.

Title Page

Abstract

Introduction

Conclusions

References

Tables

Figures



Back

Close

Full Screen / Esc

Printer-friendly Version

Interactive Discussion



about  $-0.5^{\circ}\text{C}$  over the Mediterranean Sea, and can reach between  $-1$  and  $-2^{\circ}\text{C}$  over northern Africa. The daily temporal series shows the variability of the effect of aerosols (Fig. 11b), even if the latter are constant in a month. Their effect notably depends on the presence of clouds and changes in atmospheric dynamics between the NO and PROG-M simulations (semi-direct effect).

In the PROG simulation, a similar cooling is simulated compared to the NO simulation, but the amplitude of this cooling differs from PROG-M. On average in summer 2012, the cooling at surface is weaker in PROG than in PROG-M over Europe and particularly eastern Europe, as well as in the most part of northern Africa, and inversely over regions submitted to frequent dust outbreaks such as the southwestern Mediterranean sea and the Atlantic Ocean.

The daily series of the PROG-NO difference in T2m are relatively correlated with the PROG-M-NO difference, as the correlation coefficient for the four stations considered in Fig. 11 is 0.41 in Oujda, 0.55 in Mallorca, 0.83 in Frioul and 0.68 in Lampedusa. However, the impact of some dust events can be identified in these series. For example in Oujda, AOD is higher than 0.6 between 9 and 12 July, when the maximum difference between PROG-M and NO is  $-0.5^{\circ}\text{C}$  against  $-1.0^{\circ}\text{C}$  between PROG and NO. The extra cooling of  $0.5^{\circ}\text{C}$  is likely related to the passage of the dust plume. Note that cloud cover remained weak during this period in Mallorca, enabling dust aerosols to have a strong impact on surface temperature. Similar examples have been found in Oujda (e.g. 15–18 August) and Lampedusa (9–12 July). These three stations, located in regions where average cooling is higher in PROG than in PROG-M compared to NO, reveal that the frequent dust outbreaks in clear-sky conditions are responsible for this extra average cooling.

On the contrary, in Frioul, located further to the dust sources where the average cooling is higher in PROG-M than in PROG, no such event has been identified. In addition, clear-sky conditions are often characterized by low aerosol loads (e.g. 21–23 July) where aerosol forcing is higher in PROG-M, while dust outbreaks are often affected by clouds (e.g. 18 June). Consequently, the average cooling by aerosols is

## Dust radiative effects over the Mediterranean

P. Nabat et al.

[Title Page](#)[Abstract](#)[Introduction](#)[Conclusions](#)[References](#)[Tables](#)[Figures](#)[Back](#)[Close](#)[Full Screen / Esc](#)[Printer-friendly Version](#)[Interactive Discussion](#)

reduced in PROG compared to PROG-M. However, a dynamic component could also be considered, notably to explain the strong differences in eastern Europe.

As a result, the daily variability of aerosols brought by the prognostic scheme enables to identify an extra cooling during some dust outbreaks, notably when cloud cover is not important. A comparison with surface observations is now considered. Figures 9 and 10 also present the daily averages of T2m, respectively in Lampedusa and Murcia. While PROG-M and PROG are on average cooler than NO because of the aerosol forcing, the three CNRM-RCSM5 simulations have similar temporal correlations (between 0.76 and 0.77 for Murcia, 0.72 and 0.73 for Lampedusa). Even during dust outbreaks, it is not possible to state that average temperature in PROG is closer to observations. Note however that Lampedusa island is too small to be captured by the model resolution. With regards to standard deviations, the daily variability is reduced in PROG (1.27 in Murcia, against 1.31 for PROG-M and 1.36 for NO; 0.89 in Lampedusa against 0.92 for PROG-M and 0.95 for NO). The aerosol forcing during dust events could indeed decrease the maximum daily temperature, while the effect of dust particles on thermal surface radiation (TSR) could increase night-time temperature, and thus reduce T2m diurnal variability.

Table 4 presents the scores of the evaluation of T2m for 13 stations around the Mediterranean basin (see Table 5). On average, while no change in correlation coefficient is noted, the PROG simulation is cooler than NO and PROG-M, increasing the negative bias. Nevertheless the daily variability is slightly reduced, getting closer to observed variability. In addition, it is worth mentioning ERA-Interim has the highest scores in terms of correlation and variability (standard deviation), probably benefiting from the assimilation of surface temperature (Dee et al., 2011).

#### 4.4 Sea surface temperature

Thanks to the ocean–atmosphere coupling, the aerosol-induced changes in SST can be addressed. Indeed the aerosol surface negative forcing also leads to a cooling in SST, as shown in Fig. 12, on average  $-0.4^{\circ}\text{C}$  for the difference PROG-M-NO. This

## Dust radiative effects over the Mediterranean

P. Nabat et al.

Title Page

Abstract

Introduction

Conclusions

References

Tables

Figures



Back

Close

Full Screen / Esc

Printer-friendly Version

Interactive Discussion



## Dust radiative effects over the Mediterranean

P. Nabat et al.

Title Page

Abstract

Introduction

Conclusions

References

Tables

Figures



Back

Close

Full Screen / Esc

Printer-friendly Version

Interactive Discussion



cooling is stronger near the African coast of Maghreb, where dust aerosols are prevailing in this season. This result is close to the study of Nabat et al. (2014), who have found an average aerosol effect of  $-0.6^{\circ}\text{C}$  on the Mediterranean Sea in summer. The comparison between PROG and NO shows similar differences (on average  $-0.4^{\circ}\text{C}$  as for PROG-M-NO), indicating an average similar effect of prognostic aerosols on SST. However, Fig. 12 reveals regional differences in the comparison between PROG and PROG-M. Indeed, SST is slightly warmer in the northern basins (Gulf of Lions, Adriatic Sea, Aegean Sea) in PROG than in PROG-M, and conversely colder in the Algerian basin.

This difference is also shown by the daily temporal series in the Gulf of Lions and the strait of Gibraltar (Fig. 12b). Even if both PROG-M and PROG simulate a cooling compared to NO, SST is most of the time  $0.1^{\circ}\text{C}$  warmer in PROG than in PROG-M in the Gulf of Lions. The impact of the main dust outbreaks is also noted. For example, on 18 June, under an AOD peak of 0.65, SST gets  $0.1^{\circ}\text{C}$  colder in PROG than in PROG-M which does not see this maximum. In the strait of Gibraltar, similar effects of the maximum AOD are observed (e.g. 24 June).

However the main difference between these two series is the variability of the atmospheric aerosol content. While frequent AOD peaks are observed in the Strait of Gibraltar due to frequent dust outbreaks, the latter less often reach the Gulf of Lions, hence less frequent AOD peaks. The AOD standard deviation in PROG is 0.22 for the Strait of Gibraltar and only 0.14 for the Gulf of Lions. In result, there are more days in the Strait of Gibraltar (32) where AOD is much higher (difference higher than 0.1) in PROG than in PROG-M, than in the Gulf of Lions (15), despite common averages. Consequently, the aerosol effect can be more important in the Strait of Gibraltar than in the Gulf of Lions, which must explain a cooler SST in the Strait of Gibraltar.

In addition, the days when AOD is high in the Gulf of Lions are often cloudy, which alleviate the effect of aerosols. Indeed, dust outbreaks over the northern basins are more frequent under southerly winds (Gkikas et al., 2012), that also favour humidity advection and cloud cover.

## Dust radiative effects over the Mediterranean

P. Nabat et al.

[Title Page](#)

[Abstract](#)

[Introduction](#)

[Conclusions](#)

[References](#)

[Tables](#)

[Figures](#)



[Back](#)

[Close](#)

[Full Screen / Esc](#)

[Printer-friendly Version](#)

[Interactive Discussion](#)



These comparisons have shown the effect of using a prognostic aerosol scheme, notably its importance to reproduce the daily variability of observed radiation. With regards to surface temperature, differences are also noted but they are generally too weak to see a general improvement compared to observations. Moreover, aerosol maxima over the Mediterranean are associated to particular weather conditions which are responsible for effects on radiation and temperature that are not due to aerosols. That is the reason why a composite study to isolate the effect of dust aerosols is carried out in the following section.

## 5 Composite analysis

### 5.1 Methodology

This section aims at highlighting the simulated and observed differences between days of high aerosol load and the set of all the days in terms of several meteorological parameters (radiation, temperature, cloud cover, ...). For the fourteen stations defined previously, the days of high AOD, called thereafter “dusty” days as dust aerosols are mostly responsible for these AOD maxima, have been selected over the 92 days of the summer 2012 (June-July-August). A threshold in AOD has been chosen for each station, in order to have 10 % of dusty days. This threshold differs between the model and the observations because of the model bias described in Sect. 3.1. A day is considered as a dusty day provided that AOD is higher than the defined threshold, both for the PROG simulation and observations. Days when observations were not available have been removed.

Average differences for several parameters have then been calculated between the dusty days and the set of all the days, for the three simulations (NO, PROG-M and PROG) and observations. The differences obtained for NO will enable to estimate the meteorological effect, only due to changes in weather parameters (cloud cover, wind, etc.) without considering the aerosols, for PROG-M the average effect of having an

aerosol climatology, and for PROG the adding value of prognostic aerosols. The objective is to isolate the effects of aerosols from weather changes that are systematically observed during dust outbreaks. This method is first presented for the station of Murcia, whose results are representative of the whole Mediterranean basin, and then generalized to the fourteen stations.

## 5.2 Case of Murcia

In Murcia, 9 days have been identified as dusty days over the 83 days when observations are available, results are presented in Table 6. First of all, the difference in AOD between dusty days and the set of all the days is similar in the observations and PROG, confirming the ability of CNRM-RCSM5 to reproduce aerosol daily variability, and making it possible the comparison for other parameters. In PROG-M, the slight difference ( $-0.01$ ) is due to the fact that the number of dusty days varies from one month to another (AOD is monthly constant in PROG-M); no difference in NO since no aerosols are simulated. The higher AOD during dusty days leads to a decrease in downward SSR. The difference with the set of all the days reaches  $-28 \text{ W m}^{-2}$  against only  $-8$  and  $-13 \text{ W m}^{-2}$  for respectively NO and PROG-M, while measurements in the station show a difference of  $-24 \text{ W m}^{-2}$ . The difference in NO ( $-8 \text{ W m}^{-2}$ ) can be considered as the “weather effect”, that is due to the choice of the days (meteorological and astronomical variations). The duration of sunshine indeed varies during summer, and reaches its maximum at the solstice (21 June), which can explain a part of the radiation differences in NO, in addition to changes in cloud cover. PROG-M, which has a monthly climatology of aerosols, enables to identify changes in atmospheric circulation and cloud cover due to a monthly climatology of aerosols ( $-4 \text{ W m}^{-2}$ ). The difference between PROG-M and PROG gives the contribution of the daily variability of aerosols, that is necessary to reproduce observed radiation measurements. Few changes are observed in cloud cover and TSR.

Temperature is also affected by weather changes, as dusty days are  $1.6^\circ\text{C}$  higher in NO than the set of all the days. This is probably explained by the predominance

## Dust radiative effects over the Mediterranean

P. Nabat et al.

Title Page

Abstract

Introduction

Conclusions

References

Tables

Figures



Back

Close

Full Screen / Esc

Printer-friendly Version

Interactive Discussion



**Dust radiative effects  
over the  
Mediterranean**

P. Nabat et al.

[Title Page](#)[Abstract](#)[Introduction](#)[Conclusions](#)[References](#)[Tables](#)[Figures](#)[Back](#)[Close](#)[Full Screen / Esc](#)[Printer-friendly Version](#)[Interactive Discussion](#)

of stronger southern fluxes during dusty days that can transport aerosols from Sahara to the Mediterranean basin. Figure 13 indeed shows the average circulation at 850 hPa during dusty days and the set of all the days, indicating a reinforcement of southwesterly winds in southern Spain advecting warm air. However, this increase in temperature during dusty days is lower in PROG than in PROG-M and NO, which is closer to observed variations of temperature. This decrease of  $-0.4^{\circ}\text{C}$  is caused by dust aerosols that have reduced incoming solar radiation. A similar impact is observed in soil temperature.

As a result, radiation and temperature in Murcia have been shown to be better reproduced in the PROG simulation, showing the adding value of a prognostic scheme compared to monthly climatologies to reproduce local climatic variations.

### 5.3 Generalization

A similar composite study has been carried out for other stations (defined in Table 5) where daily radiation and temperature data were available. Figure 14 presents the results per station for six parameters (AOD, solar and thermal surface radiation, cloud cover, 2 m and soil temperature) for the NO, PROG-M and PROG simulations, as well as for observations when available, while the average composites are given in Table 7.

As in Murcia, the difference in AOD between dusty days and the set of all the days is for every station similar in observations (0.23 on average) and the PROG simulation (0.22). The difference in PROG-M comes only from the number of dusty days varying from one month to another. As a consequence, measurements reveal that downward SSR is on average  $28\text{ W m}^{-2}$  lower during dusty days, which is correctly reproduced by PROG ( $-29\text{ W m}^{-2}$ ). A part of this decrease ( $-10\text{ W m}^{-2}$ ) is explained by weather changes as simulated by NO, while adding an aerosol climatology does not bring significant differences ( $-2\text{ W m}^{-2}$ ). Besides, the decrease of SSR in dusty days varies from one station to another (ranging from  $-4$  to  $-54\text{ W m}^{-2}$ ). The amplitude of the increase in AOD on dusty days and changes in weather conditions explain this variability. For

example in Mallorca, an increase of 6% in cloud cover on dusty days amplifies the dimming due to aerosol loads.

With regards to downward TSR, an average increase of  $16 \text{ W m}^{-2}$  is simulated by PROG on dusty days, but it is mainly due to weather conditions as NO and PROG-M also show an increase of  $15 \text{ W m}^{-2}$ . Dust aerosols would consequently only represent an increase of  $1 \text{ W m}^{-2}$ . Few longwave observations are unfortunately available. The only one in the Gulf of Lions shows a lower increase than simulated.

More observations are available for T2m, revealing a general increase of temperature on dusty days (on average  $1.6^\circ\text{C}$ ). As in Murcia, this increase is probably due to warm advection caused by southerly to southwesterly winds responsible of these dust outbreaks. NO indeed simulates an average increase of  $2.0^\circ\text{C}$ , but reduced to  $1.8^\circ\text{C}$  in PROG, indicating the cooling due to dust aerosols, which makes the simulation closer to observations. This improvement is noted in 9 out of the 13 stations considered in the study (Fig. 14), these 9 stations being the continental stations. The other stations either do not show a cooling (Ajaccio) or this cooling is not in line with observations (buoys of the Gulf of Lions and Azur, Lampedusa). For these three latter stations, sea surface temperature also increases on dusty days (up to  $2.0^\circ\text{C}$  in the Gulf of Lions in NO), while PROG-M and PROG both alleviate this increase by  $0.1^\circ\text{C}$ . However, this reduction cannot be confirmed by observations. Maybe the three-month period is not long enough to identify the daily effects of aerosols on SST. With regards to land soil temperature, a cooling of  $-0.4^\circ\text{C}$  due to dust aerosols is simulated by PROG, in relationship with the cooling in T2m.

## 6 Conclusions

A prognostic aerosol scheme has recently been added in the regional climate model ALADIN-Climate, enabling to have for the first time a regional coupled system model (CNRM-RCSM5) including the atmosphere, prognostic aerosols, land surface and the ocean components over the Mediterranean region. Simulations have been carried out

in summer 2012 first to evaluate the aerosols produced by the model, and then to estimate the impact of dust outbreaks on the Mediterranean climate variability.

CNRM-RCSM5 has shown its ability to reproduce the spatial and temporal variability of AOD over the Mediterranean region in summer 2012. The general spatial patterns, notably the locations of regions with high AOD, are in agreement with satellite data, while the distribution in the main different aerosol types is close to the MACC reanalysis and the independent climatology from Nabat et al. (2013). Daily variability is also correctly simulated by the model, since the evaluation against 30 stations from the AERONET network shows a mean bias of 0.02, an average correlation coefficient of 0.70 and an average ratio of standard deviations of 1.01 as good as satellite data. In addition, the TRAQA campaign has provided lidar and airborne measurements of a strong dust outbreak that occurred at the end of June 2012. The aerosol vertical distributions observed in Barcelona and in Corsica show that the model is able to reproduce the altitude of maximum extinction, even if a slight overestimation has been noted in the upper troposphere. With regards to dust size distribution, the 3-bin scheme used in ALADIN-Climate only enables to simulate higher mass concentrations for the largest particles, as well as a second maxima for submicronic particles, as observed during the TRAQA campaign.

The simulated aerosol surface shortwave DRF is negative, ranging from  $-10 \text{ W m}^{-2}$  in Europe to  $-50 \text{ W m}^{-2}$  in Africa, in line with previous studies. However, here the aerosol DRF is shown to have much variability when using a prognostic aerosol scheme instead of a monthly climatology. As a consequence, thanks to the prognostic aerosol scheme, downward SSR is better reproduced compared to ground-based measurements from several stations across the Mediterranean, both on days of high AOD (lower SSR) and low AOD (higher SSR), as correlation and standard deviation are improved. The forcing due to the dust outbreaks also causes extra cooling in surface temperature, but insufficient to improve significantly the correlation. However, the average difference between a simulation using a prognostic aerosol scheme and an aerosol climatology show a cooling of 0.1 to 0.2 °C both in T2m and SST close to the

**Dust radiative effects  
over the  
Mediterranean**

P. Nabat et al.

Title Page

Abstract

Introduction

Conclusions

References

Tables

Figures



Back

Close

Full Screen / Esc

Printer-friendly Version

Interactive Discussion



dust sources, notably in the southwestern Mediterranean. Dynamics can also change in the two simulations, and thus modify surface temperature.

A composite study has been realized in 14 stations across the Mediterranean to identify more precisely the differences between dusty days and the set of all the days.

During dusty days, SSR is shown to be reduced on average by  $28 \text{ W m}^{-2}$ , mostly because of the dimming of aerosols ( $-17 \text{ W m}^{-2}$ ) but also because of weather conditions ( $-10 \text{ W m}^{-2}$ ). In parallel, dust outbreaks that are responsible of dusty days also bring warm air, which explains that T2m is observed  $1.6^\circ\text{C}$  higher on dusty days. This warming is too strong ( $2.0^\circ\text{C}$ ) when considering only an aerosol climatology. The prognostic scheme reduces this average warming of  $0.2^\circ\text{C}$ , getting closer to observations.

Finally this study has shown the improvement brought by a prognostic aerosol scheme compared to a monthly climatology in terms of radiation and temperature during a summer. This methodology could be applied on multi-annual simulations to evaluate the impact of prognostic aerosols at the climate scale. Differences could be expected not only in terms of variability but also in average climate as suggested by the differences shown in average SST in summer 2012 in the present work.

*Acknowledgements.* We would like to thank Meteo-France for the financial support of the first author, and the surface radiation and temperature in French stations. This work is part of the Med-CORDEX initiative ([www.medcordex.eu](http://www.medcordex.eu)) and a contribution to the HyMeX and ChArMEx programmes. ChArMEx is the atmospheric component of the French multidisciplinary program MISTRALS (Mediterranean Integrated Studies at Regional And Local Scales). ChArMEx-France was principally funded by INSU, ADEME, ANR, CNES, CTC (Corsica region), EU/FEDER, Météo-France, and CEA. The aircrafts were operated by SAFIRE. TRAQA was funded by ADEME/PRIMEQUAL and MISTRALS/ChArMEx programmes and Observatoire Midi-Pyrénées. This research has received funding from the French National Research Agency (ANR) projects ADRIMED (contract ANR-11-BS56-0006) and REMEMBER (contract ANR-12-SENV-0001), as well as from the FP7 European Commission project CLIMRUN (contract FP7-ENV-2010-265192). The authors acknowledge AEMET for supplying the data and the HyMeX database teams (ESPRI/IPSL and SEDOO/Observatoire Midi-Pyrénées) for their help in accessing the data. We also thank the PI investigators of the different AERONET stations and their staff for establishing and maintaining all the sites used in the present work. The MACC

Dust radiative effects  
over the  
Mediterranean

P. Nabat et al.

Title Page

Abstract

Introduction

Conclusions

References

Tables

Figures



Back

Close

Full Screen / Esc

Printer-friendly Version

Interactive Discussion



data comes from the ECMWF website, MACC was funded between 2009 and 2011 as part of the 7th Framework Programme, pilot core GMES Atmospheric Service under contract number 218793. Measurements at Lampedusa were supported by the Italian Ministry for University and Research through Projects NextData and Ritmare. Lidar measurements in Barcelona were supported by the 7th Framework Programme project Aerosols, Clouds, and Trace Gases Research Infrastructure Network (ACTRIS) (grant agreement no. 262254); by the Spanish Ministry of Science and Innovation and FEDER funds under the projects TEC2012-34575, TEC2009-09106/TEC, CGL2011-13580-E/CLI and CGL2011-16124-E/CLI. We also thank Dominique Carrer, Xavier Ceamanos and the ICARE center for the AERUS-GEO dataset. The data of the two Mediterranean buoys were obtained from the HyMeX program, sponsored by Grants MISTRALS/HyMeX and Météo-France.

## References

- Artale, V., Calmanti, S., Carillo, A., Dell'Aquila, A., Herrmann, M., Pisacane, G., Ruti, P. M., San-  
nino, G., Struglia, M. V., Giorgi, F., Bi, X., Pal, J. S., Rauscher, S., and the PROTHEUS Group:  
An atmosphere–ocean regional climate model for the Mediterranean area: assessment of  
a present climate simulation, *Clim. Dynam.*, 35, 721–740, doi:10.1007/s00382-009-0691-8,  
2010. 25355
- Barnaba, F. and Gobbi, G. P.: Aerosol seasonal variability over the Mediterranean region and  
relative impact of maritime, continental and Saharan dust particles over the basin from  
MODIS data in the year 2001, *Atmos. Chem. Phys.*, 4, 2367–2391, doi:10.5194/acp-4-2367-  
2004, 2004. 25354
- Benedetti, A., Kaiser, J. W., and Morcrette, J.-J.: [Global climate] Aerosols [in “state of the  
climate in 2010”], *B. Am. Meteorol. Soc.*, 92, S65–S67, 2011. 25358, 25362
- Benkovitz, C. M., Scholz, M. T., Pacyna, J., Tarrason, L., Dignon, J., Voldner, E. C., Spiro, P. A.,  
Logan, J. A., and Graedel, T. E.: Global gridded inventories of anthropogenic emissions of  
sulfur and nitrogen, *J. Geophys. Res.*, 101, 29239–29253, 1996. 25359
- Bergamo, A., Tafuro, A. M., Kinne, S., De Tomasi, F., and Perrone, M. R.: Monthly-averaged  
anthropogenic aerosol direct radiative forcing over the Mediterranean based on AERONET  
aerosol properties, *Atmos. Chem. Phys.*, 8, 6995–7014, doi:10.5194/acp-8-6995-2008,  
2008. 25354

## Dust radiative effects over the Mediterranean

P. Nabat et al.

Title Page

Abstract

Introduction

Conclusions

References

Tables

Figures



Back

Close

Full Screen / Esc

Printer-friendly Version

Interactive Discussion



## Dust radiative effects over the Mediterranean

P. Nabat et al.

Title Page

Abstract

Introduction

Conclusions

References

Tables

Figures



Back

Close

Full Screen / Esc

Printer-friendly Version

Interactive Discussion



- Beuvier, J., Sevault, F., Herrmann, M., Kontoyiannis, H., Ludwig, W., Rixen, M., Stanev, E., Béranger, K., and Somot, S.: Modeling the Mediterranean Sea interannual variability during 1961–2000: focus on the Eastern Mediterranean Transient, *J. Geophys. Res.*, 115, C08017, doi:10.1029/2009JC005950, 2010. 25356
- 5 Carrer, D., Roujean, J.-L., Hautecoeur, O., and Elias, T.: Daily estimates of aerosol optical thickness over land surface based on a directional and temporal analysis of SEVIRI MSG visible observations, *J. Geophys. Res.*, 115, D10208, doi:10.1029/2009JD012272, 2010. 25360
- Colin, J., Déqué, M., Radu, R., and Somot, S.: Sensitivity study of heavy precipitation in Limited Area Model climate simulations: influence of the size of the domain and the use of the spectral nudging technique, *Tellus*, 62A, 591–604, 2010. 25356
- 10 Dee, D. P., Uppala, S. M., Simmons, A. J., Berrisford, P., Poli, P., Kobayashi, S., Andrae, U., Balmaseda, M. A., Balsamo, G., Bauer, P., Bechtold, P., Beljaars, A. C. M., van de Berg, L., Bidlot, J., Bormann, N., Delsol, C., Dragani, R., Fuentes, M., Geer, A. J., Haimberger, L., Healy, S. B., Hersbach, H., Hólm, E. V., Isaksen, I., Kallberg, P., Köhler, M., Matricardi, M., McNally, A. P., Monge-Sanz, B. M., Morcrette, J.-J., Park, B.-K., Peubey, C., de Rosnay, P., Tavolato, C., Thépaut, J.-N., and Vitart, F.: The ERA-Interim reanalysis: configuration and performance of the data assimilation system, *Q. J. Roy. Meteor. Soc.*, 137, 553–597, doi:10.1002/qj.828, 2011. 25359, 25372
- 15 Déqué, M. and Somot, S.: Extreme precipitation and high resolution with Aladin, *Idöjaras Quaterly Journal of the Hungarian Meteorological Service*, 112, 179–190, 2008. 25356
- Di Biagio, C., Di Sarra, A., and Meloni, D.: Large atmospheric shortwave radiative forcing by Mediterranean aerosols derived from simultaneous ground-based and spaceborne observations and dependence on the aerosol type and single scattering albedo, *J. Geophys. Res.*, 115, D10209, doi:10.1029/2009JD012697, 2010. 25368
- 20 Di Sarra, A., Pace, G., Meloni, D., De Silvestri, L., Piacentino, S., and Monteleone, F.: Surface shortwave radiative forcing of different aerosol types in the central Mediterranean, *Geophys. Res. Lett.*, 35, L02714, doi:10.1029/2007GL032395, 2008. 25368
- 25 Gao, X., Pal, J. S., and Giorgi, F.: Projected changes in mean and extreme precipitation over the Mediterranean region from a high resolution double nested RCM simulation, *Geophys. Res. Lett.*, 33, L03706, doi:10.1029/2005GL024954, 2006. 25356
- 30 Gibelin, A.-L. and Déqué, M.: Anthropogenic climate change over the Mediterranean region simulated by a global variable resolution model, *Clim. Dynam.*, 20, 327–339, doi:10.1007/s00382-002-0277-1, 2003. 25356

## Dust radiative effects over the Mediterranean

P. Nabat et al.

Title Page

Abstract

Introduction

Conclusions

References

Tables

Figures



Back

Close

Full Screen / Esc

Printer-friendly Version

Interactive Discussion



- Ginoux, P., Chin, M., Tegen, I., Prospero, J., Holben, B. N., Dubovik, O., and Lin, S.-J.: Sources and distributions of dust aerosols simulated with the GOCART model, *J. Geophys. Res.*, 106, 20255–20274, 2001. 25358
- Giorgi, F. and Lionello, P.: Climate change projections for the Mediterranean region, *Global Planet. Change*, 63, 90–104, doi:10.1016/j.gloplacha.2007.09.005, 2008. 25356
- Giorgi, F., Coppola, E., Solmon, F., Mariotti, L., Sylla, M. B., Bi, X., Elguindi, N., Diro, G. T., Nair, V., Giuliani, G., Cozzini, S., Guettler, I., O'Brien, T. A., Tawfik, A. B., Shalaby, A., Zakey, A. S., Steiner, A. L., Stordal, F., Sloan, L. C., and Brankovic, C.: RegCM4: model description and preliminary tests over multiple CORDEX domains, *Clim. Res.*, 52, 7–29, doi:10.3354/cr01018, 2012. 25355
- Gkikas, A., Houssos, E., Hatzianastassiou, N., Papadimas, C., and Bartzokas, A.: Synoptic conditions favouring the occurrence of aerosol episodes over the broader Mediterranean basin, *Q. J. Roy. Meteor. Soc.*, 138, 932–949, doi:10.1002/qj.978, 2012. 25354, 25361, 25373
- Gkikas, A., Hatzianastassiou, N., Mihalopoulos, N., Katsoulis, V., Kazadzis, S., Pey, J., Querol, X., and Torres, O.: The regime of intense desert dust episodes in the Mediterranean based on contemporary satellite observations and ground measurements, *Atmos. Chem. Phys.*, 13, 12135–12154, doi:10.5194/acp-13-12135-2013, 2013. 25354
- Guelle, W., Schulz, M., Balkanski, Y., and Dentener, F.: Influence of the source formulation on modeling the atmospheric global distribution of the sea salt aerosol, *J. Geophys. Res.*, 106, 27,509–27,524, 2001. 25358
- Guieu, C., Dulac, F., Desboeufs, K., Wagener, T., Pulido-Villena, E., Grisoni, J.-M., Louis, F., Ridame, C., Blain, S., Brunet, C., Bon Nguyen, E., Tran, S., Labiadh, M., and Dominici, J.-M.: Large clean mesocosms and simulated dust deposition: a new methodology to investigate responses of marine oligotrophic ecosystems to atmospheric inputs, *Biogeosciences*, 7, 2765–2784, doi:10.5194/bg-7-2765-2010, 2010. 25354
- Herrmann, M., Somot, S., Calmanti, S., Dubois, C., and Sevault, F.: Representation of spatial and temporal variability of daily wind speed and of intense wind events over the Mediterranean Sea using dynamical downscaling: impact of the regional climate model configuration, *Nat. Hazards Earth Syst. Sci.*, 11, 1983–2001, doi:10.5194/nhess-11-1983-2011, 2011. 25355, 25364
- Holben, B. N., Eck, T. F., Slutsker, I., Tanré, D., Buis, J. P., Setzer, A., Vermote, E., Reagan, J. A., Kaufman, Y., Nakajima, T., Lavenu, F., Jankowiak, I., and Smirnov, A.: AERONET-A

## Dust radiative effects over the Mediterranean

P. Nabat et al.

Title Page

Abstract

Introduction

Conclusions

References

Tables

Figures



Back

Close

Full Screen / Esc

Printer-friendly Version

Interactive Discussion



Federated Instrument Network and Data Archive for Aerosol Characterization, Remote Sens. Environ., 66, 1–16, doi:10.1016/S0034-4257(98)00031-5, 1998. 25360

Holben, B. N., Tanré, D., Smirnov, A., Eck, T. F., Slutsker, I., Abuhassan, N., Newcomb, W. W., Schafer, J. S., Chatenet, B., Lavenu, F., Kaufman, Y. J., Castle, J. V., Setzer, A., Markham, B., Clark, D., Frouin, R., Halthore, R., Karneli, A., O'Neill, N. T., Pietras, C., Pinker, R. T., Voss, K., and Zibordi, G.: An emerging ground-based aerosol climatology: aerosol optical depth from AERONET, *J. Geophys. Res.*, 106, 12067–12097, doi:10.1029/2001JD900014, 2001. 25360

Huneus, N., Schulz, M., Balkanski, Y., Griesfeller, J., Prospero, J., Kinne, S., Bauer, S., Boucher, O., Chin, M., Dentener, F., Diehl, T., Easter, R., Fillmore, D., Ghan, S., Ginoux, P., Grini, A., Horowitz, L., Koch, D., Krol, M. C., Landing, W., Liu, X., Mahowald, N., Miller, R., Morcrette, J.-J., Myhre, G., Penner, J., Perlwitz, J., Stier, P., Takemura, T., and Zender, C. S.: Global dust model intercomparison in AeroCom phase I, *Atmos. Chem. Phys.*, 11, 7781–7816, doi:10.5194/acp-11-7781-2011, 2011. 25355

Jaeglé, L., Quinn, P. K., Bates, T. S., Alexander, B., and Lin, J.-T.: Global distribution of sea salt aerosols: new constraints from in situ and remote sensing observations, *Atmos. Chem. Phys.*, 11, 3137–3157, doi:10.5194/acp-11-3137-2011, 2011. 25358

Kahn, R. A., Gaitley, B. J., Martonchik, J. V., Diner, D. J., Crean, K. A., and Holben, B.: Multiangle imaging spectroradiometer (misr) global aerosol optical depth validation based on 2 years of coincident aerosol robotic network (aeronet) observations, *J. Geophys. Res.*, 110, D10S04, doi:10.1029/2004JD004706, 2005. 25360

Kahn, R. A., Gaitley, B. J., Garay, M. J., Diner, D. J., Eck, T. F., Smirnov, A., and Holben, B. N.: Multiangle Imaging SpectroRadiometer global aerosol product assessment by comparison with the Aerosol Robotic Network, *J. Geophys. Res.*, 115, D23209, doi:10.1029/2010JD014601, 2010. 25360

Kok, J. F.: A scaling theory for the size distribution of emitted dust aerosols suggests climate models underestimate the size of the global dust cycle, *P. Natl. Acad. Sci. USA*, 108, 1016–1021, doi:10.1073/pnas.1014798108, 2011. 25359

Krzic, A., Tomic, I., Djurdjevic, V., Veljovic, K., and Rajkovic, B.: Changes in climate indices for Serbia according to the SRES-A1B and SRES-A2 scenarios, *Clim. Res.*, 49, 73–86, doi:10.3354/cr01008, 2011. 25355

Lamarque, J.-F., Bond, T. C., Eyring, V., Granier, C., Heil, A., Klimont, Z., Lee, D., Liousse, C., Mieville, A., Owen, B., Schultz, M. G., Shindell, D., Smith, S. J., Stehfest, E., Van Aar-

**Dust radiative effects  
over the  
Mediterranean**

P. Nabat et al.

Title Page

Abstract

Introduction

Conclusions

References

Tables

Figures



Back

Close

Full Screen / Esc

Printer-friendly Version

Interactive Discussion



denne, J., Cooper, O. R., Kainuma, M., Mahowald, N., McConnell, J. R., Naik, V., Riahi, K., and van Vuuren, D. P.: Historical (1850–2000) gridded anthropogenic and biomass burning emissions of reactive gases and aerosols: methodology and application, *Atmos. Chem. Phys.*, 10, 7017–7039, doi:10.5194/acp-10-7017-2010, 2010. 25359

5 Lamarque, J.-F., Shindell, D. T., Josse, B., Young, P. J., Cionni, I., Eyring, V., Bergmann, D., Cameron-Smith, P., Collins, W. J., Doherty, R., Dalsoren, S., Faluvegi, G., Folberth, G., Ghan, S. J., Horowitz, L. W., Lee, Y. H., MacKenzie, I. A., Nagashima, T., Naik, V., Plummer, D., Righi, M., Rumbold, S. T., Schulz, M., Skeie, R. B., Stevenson, D. S., Strode, S., Sudo, K., Szopa, S., Voulgarakis, A., and Zeng, G.: The Atmospheric Chemistry and Climate Model Intercomparison Project (ACCMIP): overview and description of models, simulations and climate diagnostics, *Geosci. Model Dev.*, 6, 179–206, doi:10.5194/gmd-6-179-2013, 2013. 25355

Lelieveld, J., Berresheim, H., Borrmann, S., Crutzen, P. J., Dentener, F. J., Fischer, H., Feichter, J., Flatau, P. J., Heland, J., Holzinger, R., Korrman, R., Lawrence, M. G., Levin, Z., Markowicz, K. M., Mihalopoulos, N., Minikin, A., Ramanathan, V., de Reus, M., Roelofs, G. J., Scheeren, H. A., Sciare, J., Schlager, H., Schultz, M., Siegmund, P., Steil, B., Stephanou, E. G., Stier, P., Traub, M., Warneke, C., Williams, J., and Ziereis, H.: Global air pollution crossroads over the Mediterranean, *Science*, 298, 794–799, doi:10.1126/science.1075457, 2002. 25354

20 Léon, J.-F., Augustin, P., Mallet, M., Pont, V., Dulac, F., Fourmentin, M., and Lambert, D.: Aerosol vertical distribution, optical properties and transport over Corsica (Western Mediterranean), *Atmos. Chem. Phys.*, this issue, in preparation, 2014. 25361

Levy, R. C., Remer, L. A., Mattoo, S., Vermote, E. F., and Kaufman, Y. J.: Second-generation operational algorithm: Retrieval of aerosol properties over land from inversion of Moderate Resolution Imaging Spectroradiometer spectral reflectance, *J. Geophys. Res.*, 112, D13211, doi:10.1029/2006JD007811, 2007. 25360

L'Hévéder, B., Li, L., Sevault, F., and Somot, S.: Interannual variability of deep convection in the Northwestern Mediterranean simulated with a coupled AORCM, *Clim. Dynam.*, 41, 1–24, doi:10.1007/s00382-012-1527-5, 2012. 25355

30 Lucas-Picher, P., Somot, S., Déqué, M., Decharme, B., and Alias, A.: Evaluation of the regional climate model ALADIN to simulate the climate over North America in the CORDEX framework, *Clim. Dynam.*, 41, 1117–1137, doi:10.1007/s00382-012-1613-8, 2013. 25357

**Dust radiative effects  
over the  
Mediterranean**

P. Nabat et al.

Title Page

Abstract

Introduction

Conclusions

References

Tables

Figures



Back

Close

Full Screen / Esc

Printer-friendly Version

Interactive Discussion



- Mariotti, A. and Dell'Aquila, A.: Decadal climate variability in the Mediterranean region: roles of large-scale forcings and regional processes, *Clim. Dynam.*, 38, 1129–1145, doi:10.1007/s00382-011-1056-7, 2012. 25355
- Marticorena, B. and Bergametti, G.: Modeling the atmosphere dust cycle: 1. Design of a soil-derived dust emission scheme, *J. Geophys. Res.*, 100, 16415–16430, 1995. 25358, 25359
- 5 Masson, V., Champeaux, J., Chauvin, F., Meriguet, C., and Lacaze, R.: A global database of land surface parameters at 1-km resolution in meteorological and climate models, *J. Climate*, 16, 1261–1282, 2003. 25358
- Meier, J., Tegen, I., Heinold, B., and Wolke, R.: Direct and semi-direct radiative effects of absorbing aerosols in Europe: results from a regional model, *Geophys. Res. Lett.*, 39, L09802, doi:10.1029/2012GL050994, 2012. 25355
- 10 Mlawer, E. J., Taubman, S. J., Brown, P. D., Iacono, M. J., and Clough, S. A.: Radiative transfer for inhomogeneous atmospheres: RRTM, a validated correlated-k model for the longwave, *J. Geophys. Res.*, 102, 16663–16682, 1997. 25357
- 15 Morcrette, J.-J.: Description of the Radiation Scheme in the ECMWF Model, Tech. rep., ECMWF, [http://old.ecmwf.int/publications/library/ecpublications/\\_pdf/tm/001-300/tm165.pdf](http://old.ecmwf.int/publications/library/ecpublications/_pdf/tm/001-300/tm165.pdf), 1989. 25357
- Morcrette, J.-J., Boucher, O., Jones, L., Salmond, D., Bechtold, P., Beljaars, A., Benedetti, A., Bonet, A., Kaiser, J. W., Razinger, M., Schulz, M., Serrar, S., Simmons, J., Sofiev, M., Suttie, M., Tompkins, A. M., and Untch, A.: Aerosol analysis and forecast in the european centre for medium-range weather forecasts integrated forecast system: forward modeling, *J. Geophys. Res.*, 114, D06206, doi:10.1029/2008JD011115, 2009. 25356, 25358, 25359, 25361, 25362
- 20 Moulin, C., Guillard, F., Dulac, F., and Lambert, C. E.: Long-term daily monitoring of Saharan dust load over ocean using Meteosat ISCCP-B2 data 1. Methodology and preliminary results for 1983-1994 in the Mediterranean, *J. Geophys. Res.*, 102, 16,947–16,958, 1997. 25354
- 25 Moulin, C., Lambert, C. E., Dayan, U., Masson, V., Ramonet, M., Bousquet, P., Legrand, M., Balkanski, Y. J., Guelle, W., Marticorena, B., Bergametti, G., and Dulac, F.: Satellite climatology of African dust transport in the Mediterranean atmosphere, *J. Geophys. Res.*, 103, 13137–13144, doi:10.1029/98JD00171, 1998. 25354, 25361
- 30 Nabat, P., Solmon, F., Mallet, M., Kok, J. F., and Somot, S.: Dust emission size distribution impact on aerosol budget and radiative forcing over the Mediterranean region: a regional climate model approach, *Atmos. Chem. Phys.*, 12, 10545–10567, doi:10.5194/acp-12-10545-2012, 2012. 25359

## Dust radiative effects over the Mediterranean

P. Nabat et al.

Title Page

Abstract

Introduction

Conclusions

References

Tables

Figures



Back

Close

Full Screen / Esc

Printer-friendly Version

Interactive Discussion



- Nabat, P., Somot, S., Mallet, M., Chiapello, I., Morcrette, J. J., Solmon, F., Szopa, S., Dulac, F., Collins, W., Ghan, S., Horowitz, L. W., Lamarque, J. F., Lee, Y. H., Naik, V., Nagashima, T., Shindell, D., and Skeie, R.: A 4-D climatology (1979–2009) of the monthly tropospheric aerosol optical depth distribution over the Mediterranean region from a comparative evaluation and blending of remote sensing and model products, *Atmos. Meas. Tech.*, 6, 1287–1314, doi:10.5194/amt-6-1287-2013, 2013. 25354, 25359, 25363, 25378, 25390
- Nabat, P., Somot, S., Mallet, M., Sevault, F., Chiacchio, M., and Wild, M.: Direct and semi-direct aerosol radiative effect on the Mediterranean climate variability using a Regional Climate System Model, *Clim. Dynam.*, 1–29, doi:10.1007/s00382-014-2205-6, 2014. 25354, 25355, 25357, 25358, 25367, 25370, 25373
- Noilhan, J. and Mahfouf, J.-F.: The ISBA land surface parameterisation scheme, *Global Planet. Change*, 13, 145–159, doi:10.1016/0921-8181(95)00043-7, 1996. 25356
- Papadimas, C. D., Hatzianastassiou, N., Mihalopoulos, N., Querol, X., and Vardavas, I.: Spatial and temporal variability in aerosol properties over the Mediterranean basin based on 6-year (2000–2006) MODIS data, *J. Geophys. Res.*, 113, D11205, doi:10.1029/2007JD009189, 2008. 25354
- Pappalardo, G., Amodeo, A., Apituley, A., Comeron, A., Freudenthaler, V., Linné, H., Ansmann, A., Bösenberg, J., D'Amico, G., Mattis, I., Mona, L., Wandinger, U., Amiridis, V., Alados-Arboledas, L., Nicolae, D., and Wiegner, M.: EARLINET: towards an advanced sustainable European aerosol lidar network, *Atmos. Meas. Tech.*, 7, 2389–2409, doi:10.5194/amt-7-2389-2014, 2014. 25361
- Petropoulos, G. P., Griffiths, H. M., Carlson, T. N., Ioannou-Katidis, P., and Holt, T.: SimSphere model sensitivity analysis towards establishing its use for deriving key parameters characterising land surface interactions, *Geosci. Model Dev.*, 7, 1873–1887, doi:10.5194/gmd-7-1873-2014, 2014. 25356, 25358, 25359
- Radu, R., Déqué, M., and Somot, S.: Spectral nudging in a spectral regional climate model, *Tellus*, 60A, 898–910, doi:10.1111/j.1600-0870.2008.00341.x, 2008. 25357
- Reba, M. N. M., Rocadenbosch, F., Sicard, M., Kumar, D., and Tomás, S.: On the lidar ratio estimation from the synergy between AERONET sun-photometer data and elastic lidar inversion, in: *Proc. of the 25th International Laser Radar Conference*, ISBN 978-5-94458-109-9, Saint-Petersburg (Russia), Publishing House of IAO SB RA, 5–9 July 2010, pp. 1102–1105, 2010. 25361



**Dust radiative effects  
over the  
Mediterranean**

P. Nabat et al.

[Title Page](#)[Abstract](#)[Introduction](#)[Conclusions](#)[References](#)[Tables](#)[Figures](#)[Back](#)[Close](#)[Full Screen / Esc](#)[Printer-friendly Version](#)[Interactive Discussion](#)

with Raman lidars and airborne HSRL in southern Morocco during SAMUM, *Tellus B*, 61, 144–164, doi:10.1111/j.1600-0889.2008.00390.x, 2009. 25366

5 Textor, C., Schulz, M., Guibert, S., Kinne, S., Balkanski, Y., Bauer, S., Berntsen, T., Berglen, T., Boucher, O., Chin, M., Dentener, F., Diehl, T., Easter, R., Feichter, H., Fillmore, D., Ghan, S., Ginoux, P., Gong, S., Grini, A., Hendricks, J., Horowitz, L., Huang, P., Isaksen, I., Iversen, I., Kloster, S., Koch, D., Kirkevåg, A., Kristjansson, J. E., Krol, M., Lauer, A., Lamarque, J. F., Liu, X., Montanaro, V., Myhre, G., Penner, J., Pitari, G., Reddy, S., Seland, Ø., Stier, P., Takemura, T., and Tie, X.: Analysis and quantification of the diversities of aerosol life cycles within AeroCom, *Atmos. Chem. Phys.*, 6, 1777–1813, doi:10.5194/acp-6-1777-2006, 2006. 25365

10 Todd, M. C., Karam, D. B., Cavazos, C., Bouet, C., Heinold, B., Baldasano, J. M., Cautenet, G., Koren, I., Perez, C., Solmon, F., Tegen, I., Tulet, P., Washington, R., and Zakey, A.: Quantifying uncertainty in estimates of mineral dust flux: An intercomparison of model performance over the Bodélé Depression, northern Chad, *J. Geophys. Res.*, 113, D24107, doi:10.1029/2008JD010476, 2008. 25355

15 Turuncoglu, U. U., Giuliani, G., Elguindi, N., and Giorgi, F.: Modelling the Caspian Sea and its catchment area using a coupled regional atmosphere-ocean model (RegCM4-ROMS): model design and preliminary results, *Geosci. Model Dev.*, 6, 283–299, doi:10.5194/gmd-6-283-2013, 2013. 25355

20 Valcke, S.: The OASIS3 coupler: a European climate modelling community software, *Geosci. Model Dev.*, 6, 373–388, doi:10.5194/gmd-6-373-2013, 2013. 25357

Vogel, B., Vogel, H., Bäumer, D., Bangert, M., Lundgren, K., Rinke, R., and Stanelle, T.: The comprehensive model system COSMO-ART – Radiative impact of aerosol on the state of the atmosphere on the regional scale, *Atmos. Chem. Phys.*, 9, 8661–8680, doi:10.5194/acp-9-8661-2009, 2009. 25355, 25359

25 Woodage, M. J., Slingo, A., Woodward, S., and Comer, R. E.: Simulations of desert dust and biomass burning aerosols with a high-resolution atmospheric GCM, *J. Climate*, 23, 1636–1659, doi:10.1175/2009JCLI2994.1, 2010. 25355

30 Zanis, P.: A study on the direct effect of anthropogenic aerosols on near surface air temperature over Southeastern Europe during summer 2000 based on regional climate modeling, *Ann. Geophys.*, 27, 3977–3988, doi:10.5194/angeo-27-3977-2009, 2009. 25355

Zanis, P., Ntogras, C., Zakey, A., Pytharoulis, I., and Karacostas, T.: Regional climate feedback of anthropogenic aerosols over Europe using RegCM3, *Clim. Res.*, 52, 267–278, doi:10.3354/cr01070, 2012. 25354

Discussion Paper | Discussion Paper | Discussion Paper | Discussion Paper | Discussion Paper

ACPD

14, 25351–25410, 2014

**Dust radiative effects over the Mediterranean**

P. Nabat et al.

Title Page

Abstract

Introduction

Conclusions

References

Tables

Figures

◀

▶

◀

▶

Back

Close

Full Screen / Esc

Printer-friendly Version

Interactive Discussion



## Dust radiative effects over the Mediterranean

P. Nabat et al.

Title Page

Abstract

Introduction

Conclusions

References

Tables

Figures



Back

Close

Full Screen / Esc

Printer-friendly Version

Interactive Discussion



**Table 1.** Total AOD and components for the five aerosol types simulated by CNRM-RCSM5 and the MACC reanalysis in summer 2012 over Europe (continental area up to 30° E), the Mediterranean Sea and northern Africa (continental area up to 25° N). Averages in summer from NAB13, the climatology of Nabat et al. (2013), have also been indicated with the minimum and maximum summer values (period 2003–2009). Total AOD from satellite data (MODIS, MISR, AERUS-GEO) is also given.

Europe	CNRM-RCSM5	MACC	NAB13	MODIS	MISR	AERUS-GEO
Sea-salt	0.01	0.02	0.00 [0.00–0.00]	–	–	–
Desert dust	0.04	0.06	0.05 [0.04–0.05]	–	–	–
Organic matter	0.04	0.02	0.02 [0.02–0.03]	–	–	–
Black carbon	0.01	0.01	0.01 [0.01–0.01]	–	–	–
Sulfate	0.08	0.10	0.10 [0.08–0.12]	–	–	–
Total	0.18	0.21	0.18 [0.16–0.20]	0.16	0.15	0.15
Mediterranean Sea						
Sea-salt	0.01	0.02	0.01 [0.00–0.01]	–	–	–
Desert dust	0.11	0.10	0.12 [0.10–0.13]	–	–	–
Organic matter	0.03	0.02	0.01 [0.01–0.02]	–	–	–
Black carbon	0.01	0.01	0.01 [0.00–0.01]	–	–	–
Sulfate	0.07	0.09	0.08 [0.07–0.10]	–	–	–
Total	0.23	0.24	0.23 [0.19–0.25]	0.20	0.22	0.18
Africa						
Sea-salt	0.00	0.01	0.00 [0.00–0.00]	–	–	–
Desert dust	0.37	0.18	0.31 [0.25–0.33]	–	–	–
Organic matter	0.02	0.02	0.01 [0.01–0.02]	–	–	–
Black carbon	0.01	0.01	0.01 [0.01–0.01]	–	–	–
Sulfate	0.05	0.07	0.08 [0.06–0.09]	–	–	–
Total	0.45	0.29	0.41 [0.33–0.44]	0.33	0.32	0.21

## Dust radiative effects over the Mediterranean

P. Nabat et al.

Title Page

Abstract

Introduction

Conclusions

References

Tables

Figures



Back

Close

Full Screen / Esc

Printer-friendly Version

Interactive Discussion



**Table 2.** Spatial correlation coefficients between AOD of the different datasets presented in Fig. 3.

Datasets	MODIS	MISR	AERUS-GEO	MACC
CNRM-RCSM5	0.64	0.77	0.65	0.74
MODIS		0.81	0.69	0.84
MISR			0.68	0.84
AERUS-GEO				0.61

## Dust radiative effects over the Mediterranean

P. Nabat et al.

**Table 3.** Evaluation of daily SSR simulated by NO, PROG-M, PROG and ERA-Interim against 14 ground-based measurements located around the Mediterranean basin, in terms of bias ( $W m^{-2}$ ), temporal correlation coefficient and standard deviation ratio.

Bias	MUR	BAR	MAL	ALI	AJA	CAR	MON	NIC	PER	FES	LIO	AZU	LAM	SED	MOY
NO	31.0	2.8	54.3	39.0	18.0	22.3	35.9	37.6	34.7	48.2	31.2	35.1	18.0	5.6	29.6
PROG-M	7.6	-8.5	35.1	18.1	2.4	10.1	20.8	19.6	19.3	13.6	13.6	16.6	-6.0	-13.4	10.6
PROG	9.7	-7.5	36.0	21.2	5.1	11.5	24.0	22.9	21.0	16.5	15.9	19.1	-3.5	-11.7	12.9
ERA-Interim	12.8	4.6	53.7	25.4	-1.0	-4.3	17.0	10.1	27.7	34.7	10.2	7.2	-16.8	-12.9	12.0
<b>Corr.</b>															
NO	0.72	0.76	0.66	0.62	0.87	0.89	0.71	0.67	0.76	0.39	0.87	0.86	0.81	0.84	0.75
PROG-M	0.76	0.77	0.65	0.67	0.89	0.87	0.70	0.69	0.77	0.49	0.88	0.87	0.85	0.89	0.76
PROG	0.77	0.79	0.69	0.74	0.89	0.91	0.75	0.69	0.78	0.53	0.89	0.90	0.87	0.90	0.79
ERA-Interim	0.79	0.81	0.88	0.81	0.88	0.88	0.77	0.68	0.75	0.37	0.90	0.76	0.87	0.88	0.79
<b>St. Dev.</b>															
NO	0.79	1.20	0.84	1.16	1.11	0.96	0.97	0.81	0.96	0.93	0.92	1.00	0.74	1.15	0.97
PROG-M	0.79	1.10	0.82	1.11	1.10	0.86	0.92	0.81	0.93	0.94	0.91	1.04	0.74	0.99	0.93
PROG	0.95	1.16	1.01	1.20	1.17	0.94	0.98	0.88	0.99	1.01	1.01	1.12	0.88	1.07	1.03
ERA-Interim	0.58	0.72	0.69	0.78	0.78	0.77	0.69	0.72	0.63	0.53	0.61	0.90	0.67	0.92	0.71

[Title Page](#)
[Abstract](#)
[Introduction](#)
[Conclusions](#)
[References](#)
[Tables](#)
[Figures](#)
[Back](#)
[Close](#)
[Full Screen / Esc](#)
[Printer-friendly Version](#)
[Interactive Discussion](#)


## Dust radiative effects over the Mediterranean

P. Nabat et al.

Title Page

Abstract

Introduction

Conclusions

References

Tables

Figures



Back

Close

Full Screen / Esc

Printer-friendly Version

Interactive Discussion



**Table 4.** Evaluation of daily 2 m-temperature simulated by NO, PROG-M, PROG and ERA-Interim against 13 ground-based measurements located around the Mediterranean basin, in terms of bias ( $^{\circ}\text{C}$ ), temporal correlation coefficient and standard deviation ratio.

Bias	MUR	BAR	MAL	ALI	AJA	CAR	MON	NIC	PER	FES	LIO	AZU	LAM	MOY
NO	-0.3	-1.6	1.2	-0.5	-1.5	0.9	-1.5	-0.0	-2.0	0.0	0.6	1.6	-0.4	-0.3
PROG-M	-0.6	-1.7	0.8	-0.7	-1.7	0.8	-1.7	-0.3	-2.2	-0.4	0.4	1.4	-0.8	-0.5
PROG	-0.8	-1.9	0.7	-0.8	-1.8	0.8	-1.7	-0.3	-2.2	-0.4	0.4	1.4	-0.8	-0.6
ERA-Interim	-2.7	-2.8	-1.2	-0.1	0.1	-2.8	-1.3	-1.4	-1.6	-0.9	0.4	0.6	-0.5	-1.1
<b>Corr.</b>														
NO	0.76	0.87	0.91	0.76	0.88	0.92	0.77	0.79	0.87	0.91	0.97	0.82	0.96	0.86
PROG-M	0.77	0.89	0.92	0.77	0.88	0.92	0.77	0.81	0.88	0.92	0.97	0.81	0.96	0.86
PROG	0.76	0.88	0.92	0.75	0.88	0.92	0.77	0.80	0.89	0.92	0.97	0.81	0.96	0.86
ERA-Interim	0.88	0.98	0.88	0.75	0.86	0.92	0.89	0.90	0.89	0.96	0.93	0.81	0.90	0.89
<b>St. Dev.</b>														
NO	1.36	1.09	1.25	1.44	1.45	1.16	0.90	1.42	1.37	0.96	1.14	1.08	0.97	1.20
PROG-M	1.31	1.10	1.26	1.38	1.45	1.15	0.87	1.41	1.37	0.96	1.10	1.05	0.95	1.18
PROG	1.27	1.04	1.20	1.34	1.42	1.12	0.87	1.36	1.35	0.97	1.08	1.03	0.93	1.15
ERA-Interim	1.04	0.76	0.92	1.36	1.05	1.03	0.93	0.98	0.82	0.88	0.95	0.99	1.00	0.98







## Dust radiative effects over the Mediterranean

P. Nabat et al.

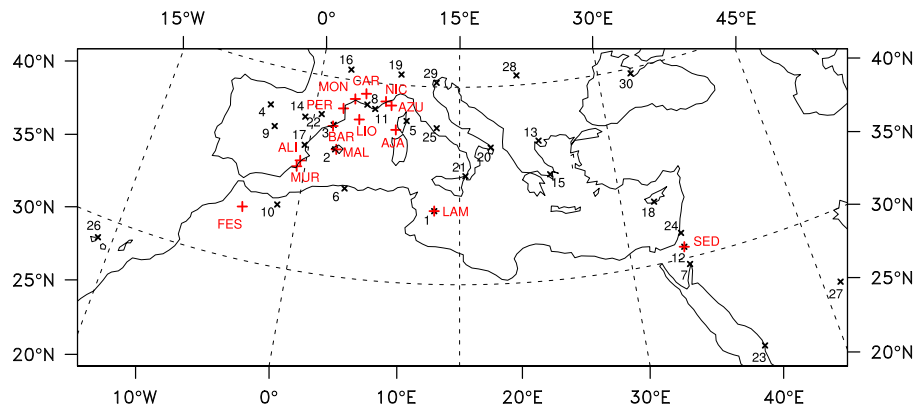


**Figure 1.** Stations of the AERONET network (black crosses, see the list of the corresponding numbers in Fig. 5). Red crosses indicate the stations providing measurements of surface radiation and temperature (see the list in Table 5).

Title Page

Abstract

Introduction

Conclusions

References

Tables

Figures



Back

Close

Full Screen / Esc

Printer-friendly Version

Interactive Discussion



## Dust radiative effects over the Mediterranean

P. Nabat et al.

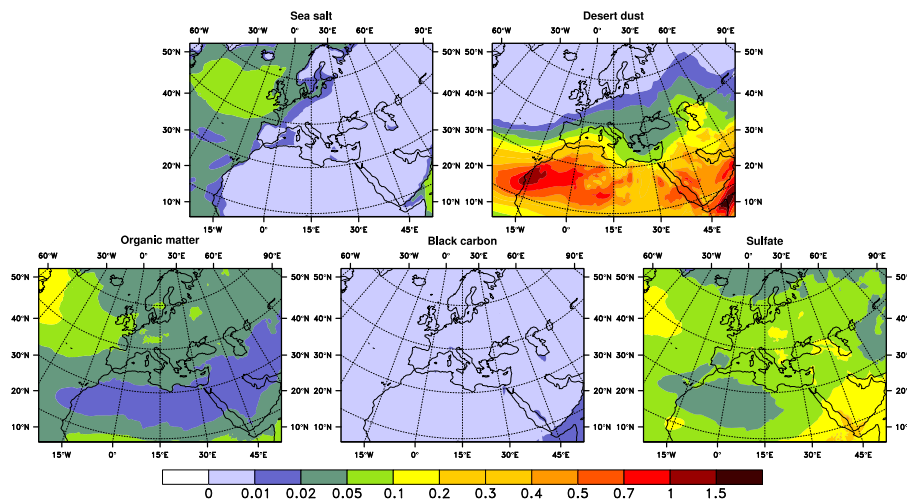


**Figure 2.** Mean aerosol optical depth at 550 nm in summer 2012 (JJA) simulated by CNRM-RCSM5 for the five aerosol types (sea-salt, desert dust, organic matter, black carbon and sulfate).

[Title Page](#)[Abstract](#)[Introduction](#)[Conclusions](#)[References](#)[Tables](#)[Figures](#)[Back](#)[Close](#)[Full Screen / Esc](#)[Printer-friendly Version](#)[Interactive Discussion](#)

## Dust radiative effects over the Mediterranean

P. Nabat et al.

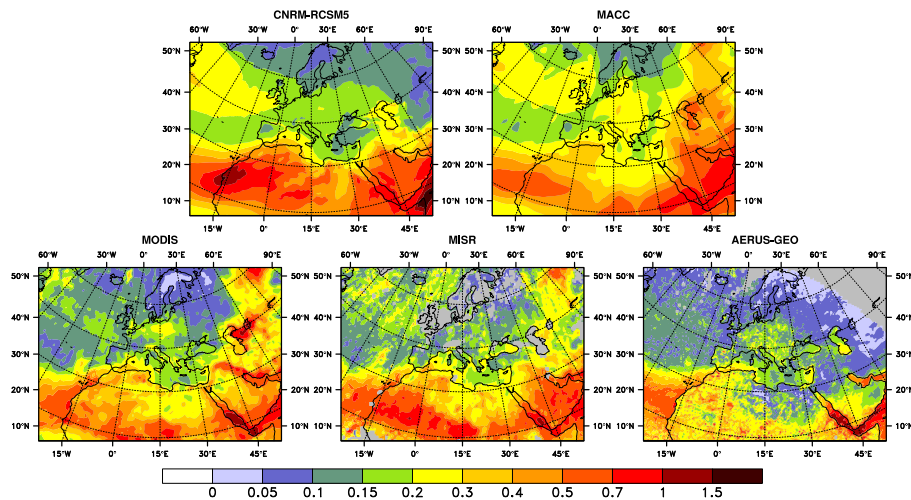


**Figure 3.** Mean aerosol optical depth at 550 nm in summer 2012 (JJA) simulated by CNRM-RCSM5 and MACC (top), and measured by 3 satellite instruments (MODIS, MISR and AERUS-GEO, bottom)

[Title Page](#)[Abstract](#)[Introduction](#)[Conclusions](#)[References](#)[Tables](#)[Figures](#)[Back](#)[Close](#)[Full Screen / Esc](#)[Printer-friendly Version](#)[Interactive Discussion](#)



## Dust radiative effects over the Mediterranean

P. Nabat et al.

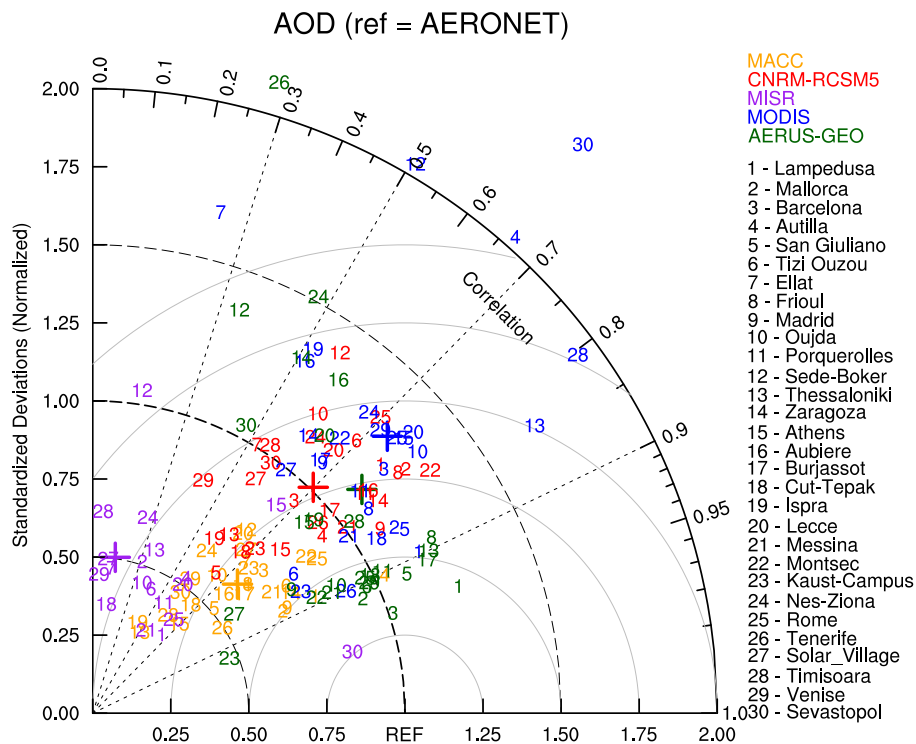


**Figure 5.** Taylor diagram evaluating CNRM-RCSM5 (red), MACC (orange) and satellite (MODIS, blue and AERUS-GEO, green) data against 30 AERONET ground-based observations in terms of daily AOD in summer 2012. Averages over the 30 stations for each dataset are indicated with crosses.

Title Page

Abstract

Introduction

Conclusions

References

Tables

Figures



Back

Close

Full Screen / Esc

Printer-friendly Version

Interactive Discussion





## Dust radiative effects over the Mediterranean

P. Nabat et al.

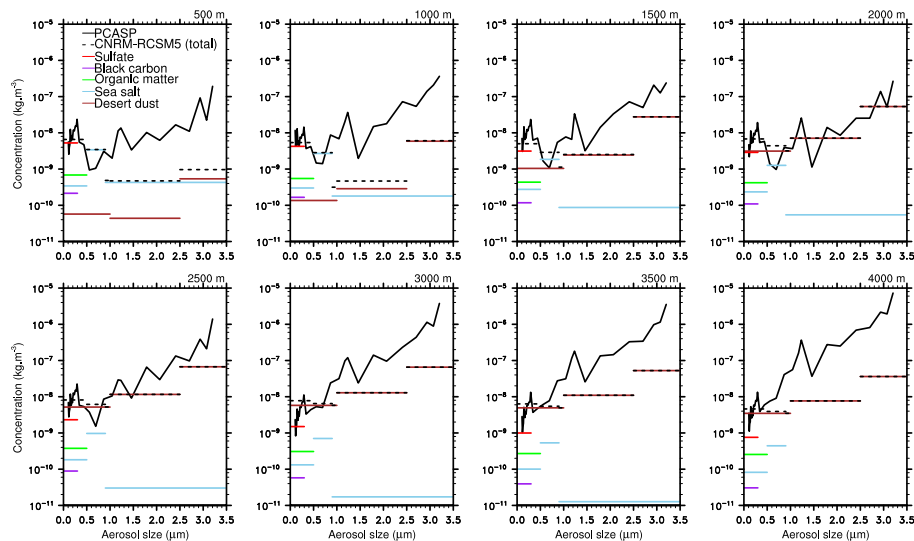


**Figure 7.** Dust particle size distribution observed by the PCASP instrument onboard ATR42 (flight 22) on 29 June at 8 UTC (black lines), the dust refractive index has been adjusted (1.53–0.002i). Colored lines indicate the aerosol concentration for each aerosol bin of CNRM-RCSM5.

Title Page

Abstract

Introduction

Conclusions

References

Tables

Figures



Back

Close

Full Screen / Esc

Printer-friendly Version

Interactive Discussion



## Dust radiative effects over the Mediterranean

P. Nabat et al.

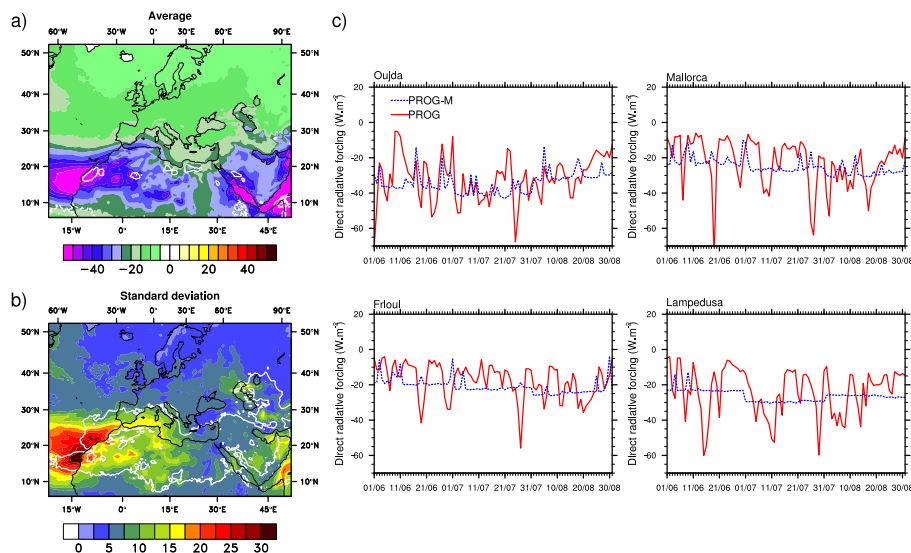


**Figure 8.** Aerosol shortwave direct radiative forcing (DRF) in the PROG and PROG-M simulations. **(a)** Average in summer 2012 for PROG (colors) and the PROG-PROG-M difference (white lines, interval is  $5 \text{ W m}^{-2}$ ). **(b)** Standard deviation of daily DRF for PROG (colors). The white line indicated the region where the ratio between the standard deviations of PROG and PROG-M is higher than 2. **(c)** Daily series for PROG (red) and PROG-M (blue) over the 4 AERONET stations defined in Fig. 4.

Title Page

Abstract

Introduction

Conclusions

References

Tables

Figures



Back

Close

Full Screen / Esc

Printer-friendly Version

Interactive Discussion



Dust radiative effects  
over the  
Mediterranean

P. Nabat et al.

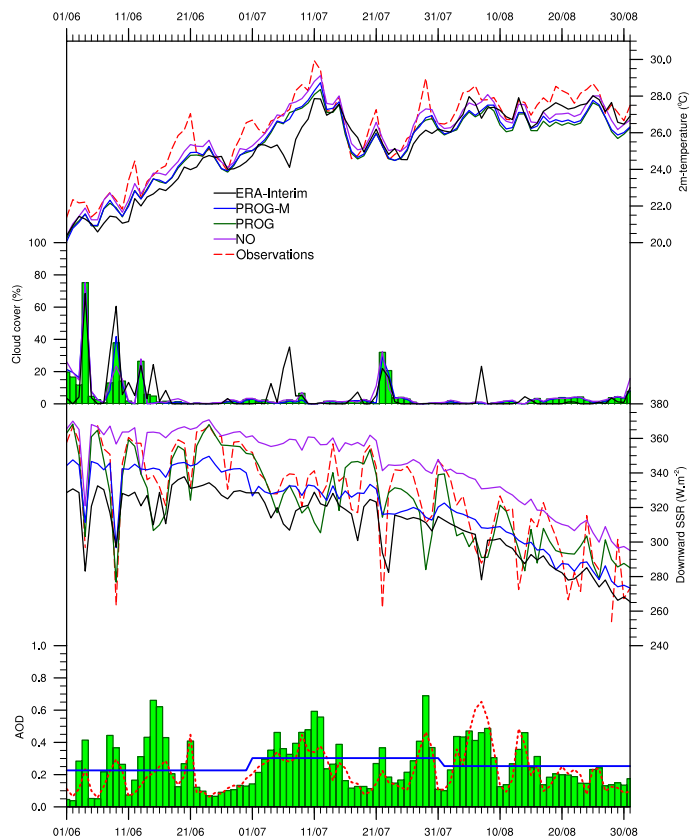


**Figure 9.** 2 m-temperature ( $^{\circ}\text{C}$ , curves), cloud cover (% , green bars for PROG, curves for the other simulations), downward SSR ( $\text{W m}^{-2}$ , curves) and AOD (green bars for PROG, blue line for PROG-M), from top to bottom, in Lampedusa (Italy) for PROG (green), PROG-M (blue), NO (purple), ERA-Interim (black) and observations (dashed red).

[Title Page](#)[Abstract](#)[Introduction](#)[Conclusions](#)[References](#)[Tables](#)[Figures](#)[Back](#)[Close](#)[Full Screen / Esc](#)[Printer-friendly Version](#)[Interactive Discussion](#)

**Dust radiative effects over the Mediterranean**

P. Nabat et al.

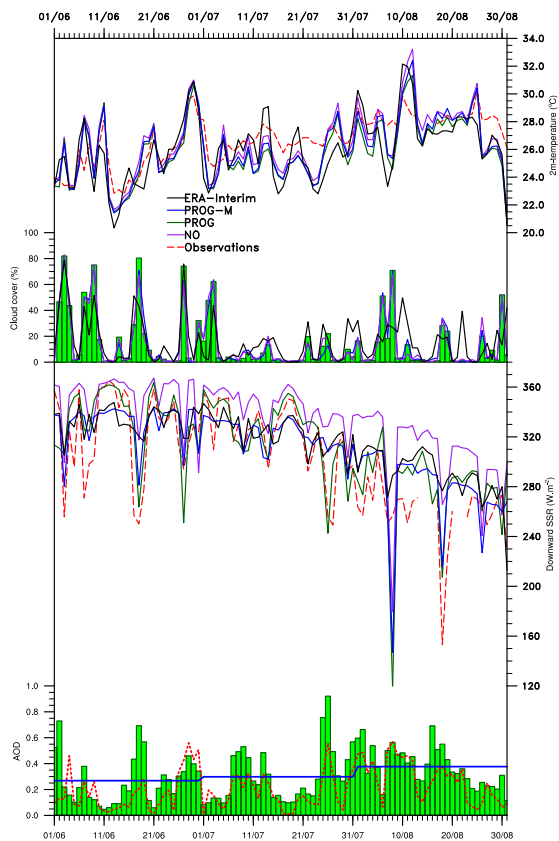


**Figure 10.** Same as Fig. 9 but for Murcia (Spain).

Title Page

Abstract

Introduction

Conclusions

References

Tables

Figures



Back

Close

Full Screen / Esc

Printer-friendly Version

Interactive Discussion



## Dust radiative effects over the Mediterranean

P. Nabat et al.

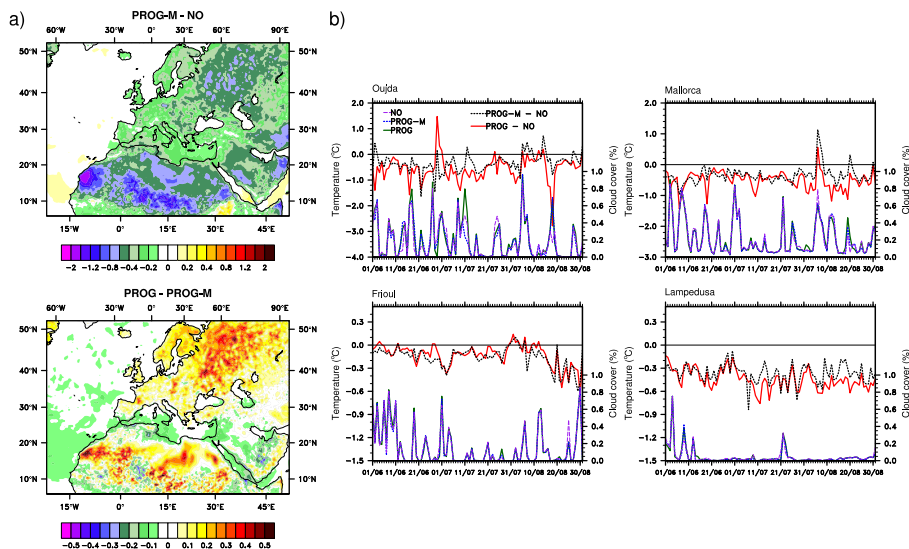


**Figure 11.** Impact of aerosols on 2 m-temperature ( $^{\circ}\text{C}$ ) in the PROG and PROG-M simulations. **(a)** Average in summer 2012 for the PROG-M-NO (top) and PROG-PROG-M (bottom) differences. **(b)** Daily series for the PROG-NO (red) and PROG-M-NO (blue) 2 m-temperature differences over the 4 AERONET stations defined in Fig. 4. Cloud cover has been added in grey lines for NO (dashed line), PROG-M (dotted line) and PROG (full line).

Title Page

Abstract

Introduction

Conclusions

References

Tables

Figures



Back

Close

Full Screen / Esc

Printer-friendly Version

Interactive Discussion



## Dust radiative effects over the Mediterranean

P. Nabat et al.

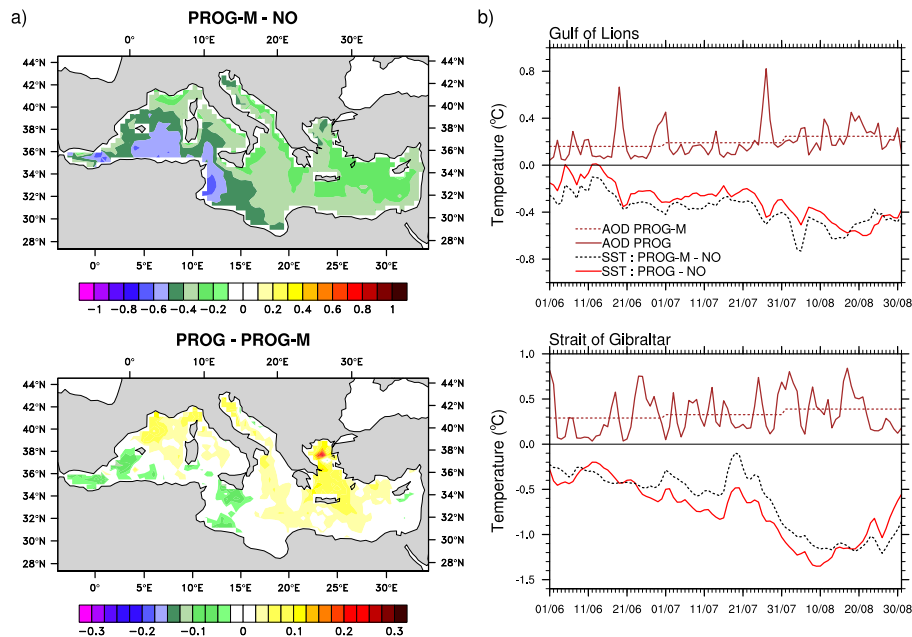


**Figure 12.** Impact of aerosols on SST ( $^{\circ}\text{C}$ ) in the PROG and PROG-M simulations. **(a)** Average in summer 2012 for the PROG-M-NO (top) and PROG-PROG-M (bottom) differences. **(b)** Daily series for the PROG-NO (red) and PROG-M-NO (blue) differences over the Gulf of Lions (top) and the strait of Gibraltar (bottom).

**Dust radiative effects  
over the  
Mediterranean**

P. Nabat et al.

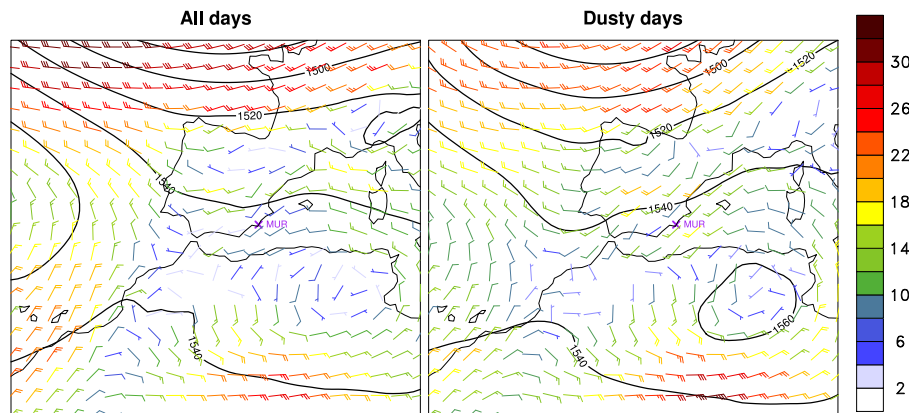


**Figure 13.** Average wind ( $\text{km h}^{-1}$ , colored barbs) and geopotential (mgp, black lines) at 850 hPa for the set of all the days (left) and the dusty days (right) defined in Murcia.

[Title Page](#)[Abstract](#)[Introduction](#)[Conclusions](#)[References](#)[Tables](#)[Figures](#)[Back](#)[Close](#)[Full Screen / Esc](#)[Printer-friendly Version](#)[Interactive Discussion](#)

Dust radiative effects over the Mediterranean

P. Nabat et al.

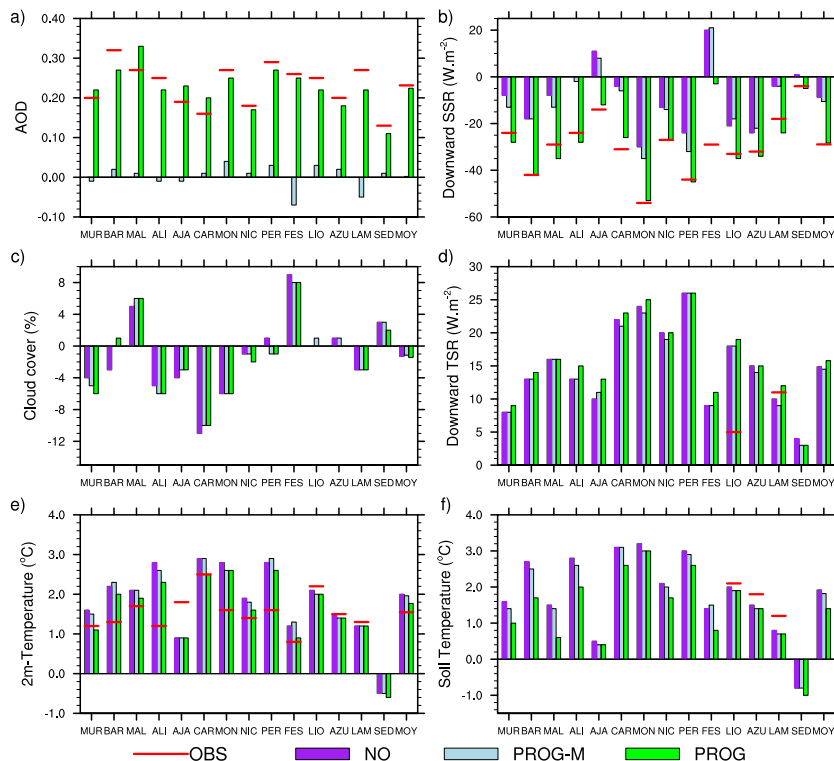


**Figure 14.** Average AOD (a), downward SSR (b), cloud cover (c), downward TSR (d), 2 m-temperature (e) and soil temperature (f) difference between the dusty and the set of all the days in fourteen stations (Murcia, Barcelona, Carpentras, Ajaccio, Fès, Mallorca and the buoy in the Gulf of Lions) in summer 2012 for the NO, PROG-M and PROG simulations, as well as observations (AERUS-GEO for AOD, ground-based measurements for the other parameters). For Lampedusa and the buoys in the Gulf of Lions and Azur, 2 m-temperature has been replaced by SST.

Title Page	
Abstract	Introduction
Conclusions	References
Tables	Figures
◀	▶
◀	▶
Back	Close
Full Screen / Esc	
Printer-friendly Version	
Interactive Discussion	

